Available online at www.CivileJournal.org

Civil Engineering Journal

(E-ISSN: 2476-3055; ISSN: 2676-6957)

Vol. 11, No. 03, March, 2025

Performance Optimization of Masonry Mortar with Marble Dust, Spent Coffee Grounds, and Peanut Shell Ash

Alexey N. Beskopylny [1*], Mohammad Hematibahar [2], Komeil Momeni [3], Sergei A. Stel'makh [4], Evgenii M. Shcherban' [5]

[1] *Department of Transport Systems, Faculty of Roads and Transport Systems, Don State Technical University, 344003 Rostov-on-Don, Russia.*

[2] *Department of Reinforced Concrete and Stone Structures, Moscow State University of Civil Engineering, 129337, Moscow, Russia.*

[3] *Department of Civil Engineering, National University of Skills (NUS), Tehran, Iran.*

[4] *Department of Unique Buildings and Constructions Engineering, Don State Technical University, 344003 Rostov-on-Don, Russia.*

[5] *Department of Engineering Geometry and Computer Graphics, Don State Technical University, 344003 Rostov-on-Don, Russia.*

Received 26 December 2024; Revised 23 February 2025; Accepted 27 February 2025; Published 01 March 2025

Abstract

This research focused on the inclusion of spent coffee grounds (SCGs) and peanut shell ash (PSH) as variable additives and marble dust as a constant additive to cement materials to substitute aggregates and determine the effect of each variable on the properties of cement materials. To determine the influence of PSH and SCGs, these were added to mortar in 0.1, 0.2, and 0.3% proportions and were combined with microsilica and superplasticizer. To analyze the results, the compressive and flexural strengths during three-point bending were investigated. The chemical composition and microstructure of the mortar mix were investigated using Scanning Electron Microscopy (SEM) and Energy-Dispersive X-ray (EDX) spectroscopy. The results showed that incorporating microsilica into the mortar mix increased the compressive strength to over 35.42 MPa compared to the control sample's 33.4 MPa. Adding 0.1% and 0.3% of SCGs and PSH improved the compressive strength of the mortar mix to over 39.48 and 38.09 MPa, respectively. Including 0.2% SCGs and 0.1% PSH increased the flexural strength to over 4.52 and 6.0 MPa, respectively. The SEM and EDX results showed that adding 0.3% SCGs slowed down the formation of calcium silicate hydrates (C-S-H), consequently slowing down the hydration processes, and the strength gain was slower compared to microsilica. The addition of 0.3 PSH stimulated the formation of C-S-H, additionally supplying the cement matrix with such elements as Si and Al. Overall, adding SCGs and PSH has a positive effect on the mechanical and chemical properties of the mortar mix, although adding PSH is more beneficial than adding SCGs.

Keywords: Cement; Mortar; Scanning Electron Microscope (SEM); Energy-Dispersive X-Ray; Spent Coffee Grounds; Peanut Shell; Compressive Strength; Flexural Strength.

1. Introduction

Improving the load-bearing capacity of concrete using materials like fibers, nano-additives, and structural reinforcement is a significant trend in the construction industry [1]. For example, incorporating fibers at varying volume fractions is a good way to enhance concrete's mechanical properties [2]. Several studies have explored using Trichoderma Reesei fungi to boost the compressive strength of self-healing concrete. Another way to improve the mechanical properties of concrete is reinforcement using 3D-printed structures [3–5].

* Corresponding author: besk-an@yandex.ru

http://dx.doi.org/10.28991/CEJ-2025-011-03-09

Meanwhile, many studies have focused on improving the mechanical or chemical properties of concrete by adding organic materials to cement [5, 6]. To explore how organic materials can enhance concrete, Pan et al. [7] investigated the effects of carrot extract on tunneling concrete. The authors found that carrot extract can increase the compressive and tensile strengths of concrete by more than 20.8% and 36.5%, respectively. Furthermore, the authors recognized that incorporating carrot extract into tunnel concrete enhanced hydration more effectively than incorporating it into traditional concrete. In fact, some scientists want to use waste materials to improve the mechanical properties. In another example, Hakeem et al. [8] examined the impact of adding nano-sesame stalk ash (NSSA) and rice straw ash (RSA), which are by-products of bio-energy production, to High-Strength Concrete (HSC). They found that when 20% of RSA and 5% of NSSA were added to concrete, the compressive strength improved to 88.9 and 90.7 MPa, respectively. In another example, researchers added fulvic acid and humic acid as organic additives to concrete. It was found that the curing time of reinforced concrete with these acids increased. Two other types of organic materials were added to concrete: wheat straw and corncob granules. These two concrete compositions had a higher performance than other types of concrete with added organic materials [9, 10]. Liu et al. used rice husks, sawdust, and the grains of corn distillers and unhulled rice distillers as four materials to reinforce concrete. The study showed a reduction in concrete porosity when organic materials were added [11].

Siddique [12] added wood ash to concrete to find the mechanical and chemical properties of concrete. Higher wood ash percentages correlated with lower flexural and compressive strengths. D'Eusanio et al. [10] explored the use of apricot (AS), peach (PS), and plum shells as sustainable aggregates in lightweight non-structural concrete, characterizing its mechanical and chemical properties. Concrete containing additional AS exhibited the highest compressive and flexural strengths. According to the results, the compressive strength of concrete when AS was added to it was over 6.98 MPa, and its flexural strength was more than 7.71 MPa. Traore et al. [13] attempted to find the mechanical properties of concrete when oil palm shells (OPSs) were added to it. Its compressive and flexural strengths decreased by over 18% with the addition of OPSs. However, these materials can improve concrete's mechanical properties, while peanut shell (PSH), spent coffee grounds (SCGs), and marble dust are more available in the world.

For example, peanut shell (PSH) is a by-product of the removal of groundnuts and has a very slow decomposition as an agricultural and industrial waste product. It not only has various bioactive and functional components but also has many commercial advantages. For instance, it serves as a raw material, food source, fertilizer filler, and even bio-filter medium; however, significant PSH volumes are incinerated or landfilled, contributing to environmental pollution [14, 15]. PSH, a by-product of agriculture and industry, annually contributes over a million tons of waste to the environment. These shells are rich in lignin and degrade slowly in the natural environment. Due to its fibrous nature and widespread availability, PSH serves as a valuable additive for cement and concrete [16].

When coffee was discovered in Ethiopia about 1000 years ago, many of its benefits were uncovered. As coffee consumption is a habit around the world and coffee consumption has increased, global coffee consumption in 2015/2016 was equivalent to 151.3 million 60 kg bags, and more than 90% of brewed coffee ended up as so-called spent coffee grounds (SCGs) [17, 18]. The widespread availability of SCGs worldwide allows for their use as a cement and concrete additive, demonstrating a noticeable effect. Since this study examines the effect of adding PSH and SCGs to concrete and cementitious materials, the literature review in this section focuses on this type of concrete. As an example, Roychand et al. [19] attempted to add SCGs to concrete to increase its mechanical properties, finding that its compressive strength decreased. Na et al. [20] attempted to add the activated carbon manufactured from waste coffee grounds. They added coffee grounds to cement in 0.5, 1, 1.5, 5, and 10% weight fractions. Their results showed that the compressive strength decreased, but a weight fraction of 10% of the coffee grounds had the best results compared to other percentages. Mohamed & Djamila [21] added the coffee grounds to concrete with 0, 5, 10, 15, and 20% by volume of the sand. They found that the thermal characteristics improved when 15 and 20% of coffee grounds by volume of the sand were added to concrete. Most investigations indicate that adding coffee grounds to concrete reduces its compressive strength. In addition, adding peanut shell achieves different mechanical properties. For example, Horma et al. [22] added crushed PSH to concrete from 0 to 6%. They found that this not only improved the thermal condition of concrete but also had a direct effect on the mechanical properties of concrete. In another study, PSH was replaced by cement in percentages of 5, 10, 15, 20, and 25%. According to the results, after 28 days of curing in sulfuric acid, the compressive strength decreased more than 0.18% when 10% of GSA was added to concrete [23]. Usman et al. [24] added PSH to cement pastes in percentages from 0 to 50%, finding the best percentage to be 10%. The literature review on the addition of PSH to concrete and cementitious materials showed that 10% of additional PSH can significantly improve the mechanical properties, such as compressive strength and thermal performance, of concrete.

Marble dust is usually used as a material to replace cement or sand to reduce natural hazards, and it can be combined with agricultural waste [25]. Adding marble dust to cement material and concrete can improve durability and compressive strength. The maximum compressive strength reached when marble dust was added to concrete was more than 10% [26].

Microsilica can improve the mechanical properties of concrete and cement material due to the creation of C-S-H after hydration in cement. Shooshpasha et al. [27] studied the effect of sand–cement–silica fume samples with different percentages. Their research revealed a positive correlation between the proportion of silica fume and the mechanical properties of the concrete. In another experiment, Shooshpasha et al. [28] determined what percentages of silica fume fill or close the pores of sand–cement mixtures. This method can help improve the mechanical properties and durability of cementitious materials.

Superplasticizer (S.P.) can reduce the amount of water usage and improve the mechanical properties of concrete at the same time, provided that the ratio of S.P. to water is controlled [29]. Overall, the addition of S.P. can improve the mechanical properties and reduce the porosity of concrete while not affecting the hydration [30].

Thus, there are already many studies examining the effects of SCGs and PSH, as well as marble dust and microsilica separately. That is, the positive and negative effects of adding these components separately to concrete are already known [14, 15, 19, 26, 28]. However, gaps have been identified in the literature regarding the study of the use of a complex of such additives. There are very few studies examining the use of several types of additives from industrial and agricultural waste (three or more) in concrete, complementing each other and multiplying the effect [31-34]. The use of marble dust in combination with SCGs and PSH when replacing part of the cement or fine aggregates will reduce the overall carbon footprint of the material. This approach is in line with modern trends in green construction, where minimizing cement consumption while maintaining structural integrity is a key goal. Ultimately, the use of SCGs and PSH in this study offers a unique balance between strength enhancement, sustainability, and durability, making them an excellent alternative to many traditional biowaste additives.

To systematically analyze the impact of SCGs and PSH on cementitious materials, this paper is structured as follows. First, the Materials and Methods section describes the composition of the mortar mix, including the types and proportions of cement, marble dust, microsilica, superplasticizer, SCGs, and PSH (0.1, 0.2, and 0.3%), along with the experimental procedures for sample preparation and testing. Next, the Results and Discussion section presents the mechanical properties of the mortar, including compressive and flexural strengths, supported by stress–strain curves and statistical analysis. The Fracture Mode Analysis section follows, investigating the failure mechanisms of different mixtures under load, while the Scanning Electron Microscope (SEM) and Energy-Dispersive X-Ray (EDX) Analysis section explores the microstructural and chemical changes induced by the additives. Finally, the Discussion section contextualizes the findings within the literature, and the Conclusion summarizes key takeaways and suggests avenues for future research.

2. Materials and Methods

2.1. Materials

To mix concrete, ordinary Portland cement, tap water, marble dust, microsilica, and superplasticizer (S.P) were used. PSH and SCGs were added with percentages of 0.1, 0.2, and 0.3% to the mortar mix. The amount of S.P and water was changed according to the change in the percentage of PSH and SCGs (Table 1). Figure 1 shows the microsilica microstructure obtained by Field Emission Scanning Electron Microscopy (FESEM) (maximum of 150 nm and minimum of 72 nm). Table 2 shows the chemical composition of microsilica via X-ray fluorescence analysis (XRF) through a Philips (company) PW 2404 (Model) device.

Table 1. Mixture design of concrete samples

Samples	Cement (kg/m^3)	Water (kg/m^3)	Marble Dust (kg/m^3)	PSH (kg/m^3)	SCG (kg/m^3)	Microsilica (kg/m^3)	S.P (kg/m^3)
C	550	176	1300	-	-	-	27.5
M.S	450	148.5	1300	-	-	100	24.75
C-1	450	148.5	1300	-	13.5 (0.1%)	100	24.75
C-2	450	148.5	1300	-	27 (0.2%)	100	27
C-3	450	148.5	1300	-	40.5 (0.3%)	100	29.25
P-1	450	148.5	1300	13.5 (0.1%)	-	100	27
P-2	450	148.5	1300	27 (0.2%)	-	100	29.25
P-3	450	148.5	1300	40.5 (0.3%)	-	100	31.5

* PSH: peanut shell, SCG: spent coffee ground, S.P: superplasticizer.

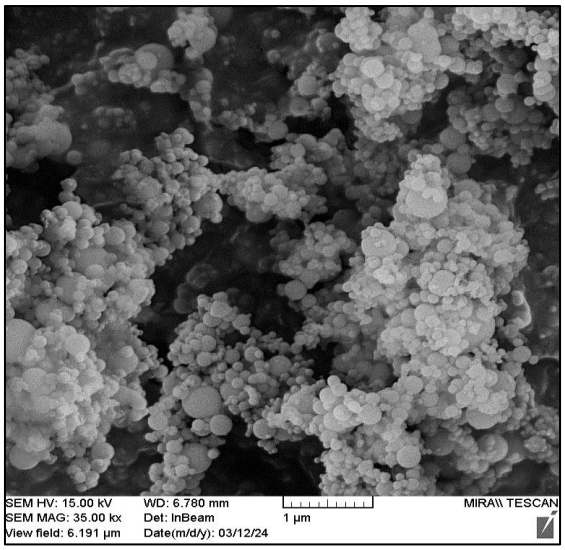

Figure 1. SEM results of microsilica

Table 2. Chemical composition of microsilica

Materials	Chemical Composite (%)
SiO_2	91.55
Al_2O_3	1.024
K_2O	1.73
MgO	1.02
Na_2O	0.52
Fe_2O_3	0.59
CaO	0.45
SO_3	0.35
P_2O_3	0.14
Cl	0.105
MnO	0.074
Zn	0.014
Pb	0.009
Rb	0.005
Sr	0.005
Cu	0.003
Ga	0.002
L.O. I	2.37

2.2. Methods

This research investigated the influence of two variables, PSH and SCGs, on the alterations in mechanical properties. Accordingly, both PSH and SCGs were added to the mortar mix in percentages of 0.1, 0.2, and 0.3%. To understand the cause-and-effect relationship, SEM and EDX were performed to determine the fractured surface and chemical composition of the cement.

The following initial hypotheses of reinforced concrete with PSH and SCGs were made.

SCG: When SCGs are added to cement material, hydration increases faster. Although the inclusion of SCGs in the mortar mix can improve the mechanical properties, the greatest effect of SCGs is on the microstructure behavior.

PSH: The addition of PSH can improve the compressive and flexural strengths due to the nature of the fibers, which gives the best results as the performance of the cement beam is improved.

This research attempted to prove these two initial hypotheses. In addition, due to the use of marble dust, PSH, and SCGs, this cementitious material is known to be sustainable. We attempted to replace this cementitious material with waste material aggregates such as marble dust, fillers such as SCGs, and fibers such as PSH (Figure 2).

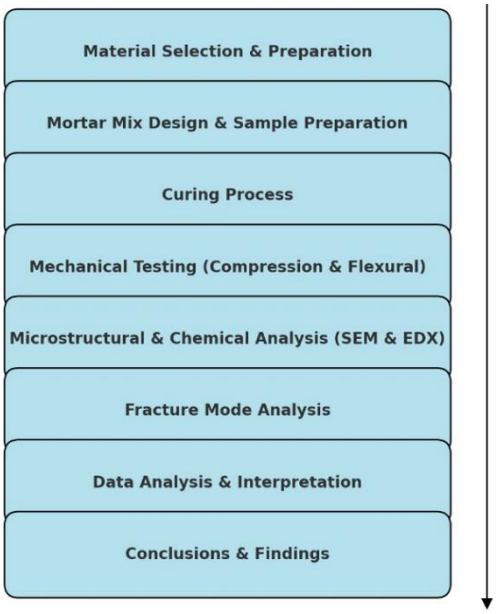

Figure 2. Methodology of current study

2.3. Laboratory and Experimental Methods

For cement samples, all materials were first weighed and then mixed together. The mixing order was as follows: marble dust, cement, and microsilica were first mixed until a homogeneous mixture was obtained, PSH or SCGs were added, and the mixture was mixed again until a homogeneous mixture was obtained before adding water. Finally, water was added to the mixture. After adding S.P., mixing was continued. In general, the mixing process continues for more than 15 minutes with a manual cement mixer.

Following the mixing process, compression cubes and flexural bending prisms were filled with cementitious materials. Two mechanical experiments were performed to find the compressive and flexural strengths of the cementitious materials. All samples were tested more than three times. Compressive strength was determined according to ASTM C109 with the dimensions of 50×50×50 mm, and flexural strength was determined according to GB/T 17671 using three-point bending experiments with the dimensions of 160×40×40 mm [35, 36].

3. Results

3.1. Compressive Strength

Initially, the compressive strength results of cementitious materials with and without microsilica were compared, as shown in Table 3. Subsequently, the remaining samples were analyzed.

Table 3. Compressive strength of control sample and control sample with microsilica

Sample	Compressive Strength (MPa)	Average of Compressive Strength (MPa)	Maximum Strain	Error (MPa)
C (1)	33.63	33.4	0.64	± 0.37
C (2)	32.95		0.63	
C (3)	33.61		0.75	
M.S (1)	35.31	35.42	0.063	± 0.86
M.S (2)	34.61		0.055	
M.S (3)	36.34		0.056	

According to Table 3, the compressive strength of C (control sample) was more than 33.4 MPa, and when microsilica was added to the control sample, the compressive strength of MS increased to more than 35.42 MPa. According to the table, the maximum strain values for the C samples surpassed those of the MSs. Figure 3 shows the stress–strain compressive strength. It is found that the MSs have stronger elastic behavior than the C samples do. Nevertheless, the MSs demonstrate sudden failure because of the straining softening process.

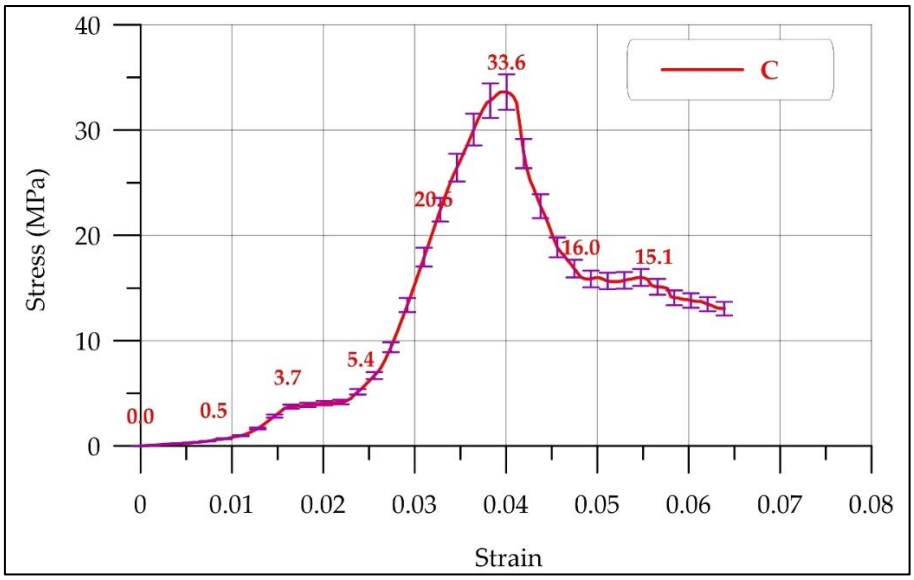

(a)

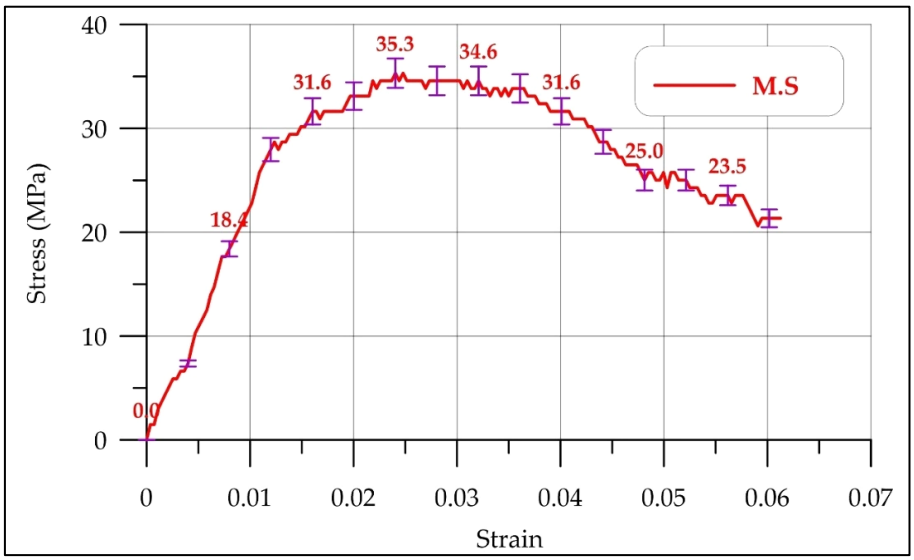

(b)

Figure 3. Stress–strain curve: (a) control sample; (b) control sample with microsilica

Figure 3 shows a peak stress point at 33.6 MPa, which represents the maximum compressive strength of the control sample. A post-peak softening region, where the material experiences gradual failure and load redistribution, is shown. The curve also includes error bars that indicate variations in the experimental data. The strain at peak stress (~0.04) highlights the stiffness and ductility behavior of the mortar. This stress–strain curve helps in evaluating the mechanical response of the control mixture before comparing it with the modified mortar samples containing SCGs and PSH.

According to Table 3, the average compressive strength of the control sample (C) is 33.4 MPa. The MS, which contains microsilica, shows an average compressive strength of 35.42 MPa.

The increase in strength (~6%) in the MS confirms that microsilica enhances the cementitious bond by improving C-S-H formation [37].

The strain values show that the MS has a greater elastic response than the control sample does, indicating better structural integrity. The table also includes error margins, which assure the reliability of the results. Figure 3 visually illustrates the mechanical behavior, while Table 3 quantitatively presents the strength values. As can be seen in the table, the addition of microsilica increases the compressive strength.

SCGs with 0.1, 0.2, and 0.3% percentages were added to cementitious materials. Considering the results of C-1 (cementitious material with 0.1% of SCGs added), the compressive strength was more than 39.48 MPa, while the strain was 0.06. This shows that adding 0.1% of SCGs increases the compressive strength compared to adding M.S. and C. samples. As illustrated in Figure 4-a, the elastic deformation of the concrete, as depicted by the C-1 stress–strain curve, shows a gradual increase.

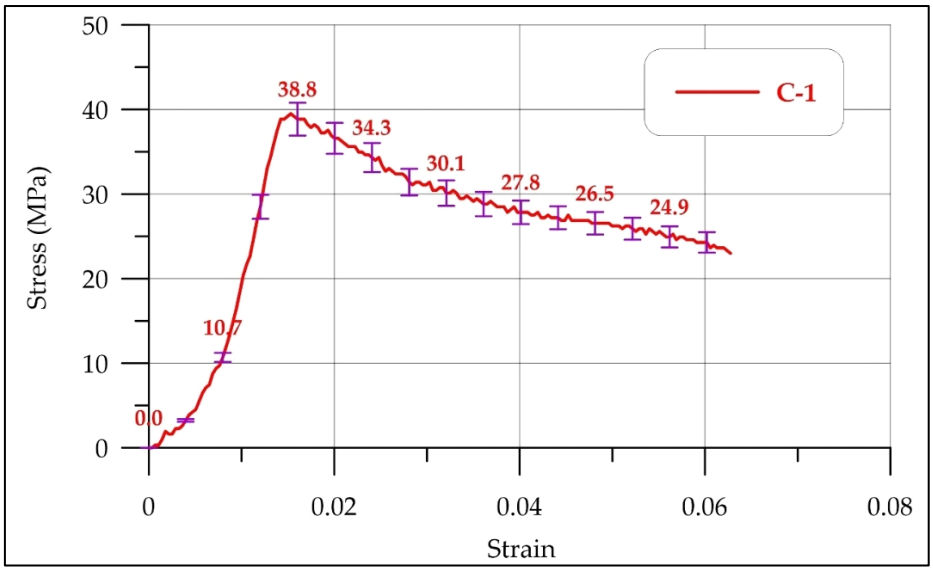

(a)

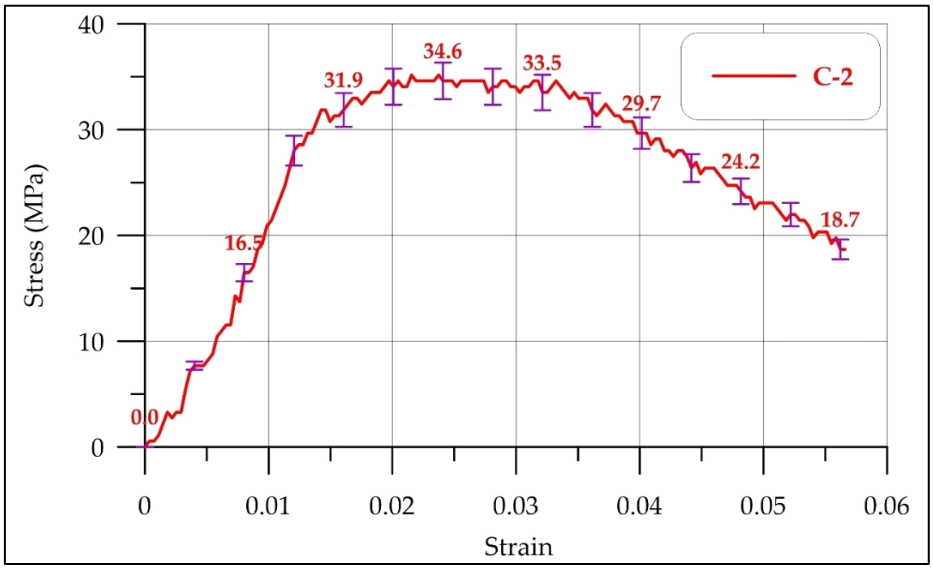

(b)

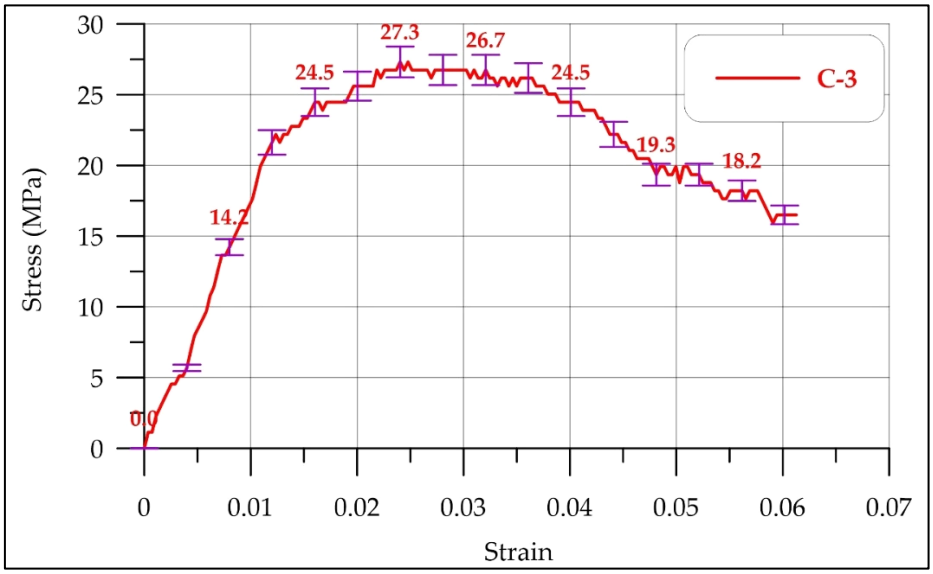

(c)

Figure 4. Compressive strength: (a) C-1 with addition of 0.1% of SCGs; (b) C-2 with addition of 0.2% of SCGs; (c) C-3 with addition of 0.3% of SCGs

When 0.2% (C-2) of SCGs was added to the cementitious materials, the compressive strength decreased to more than 35.53 MPa, the error was ±0.88, and the maximum strain was more than 0.056. The stress–strain curve shows the process of strain softening after the maximum stress to the ultimate strain (Figure 4-b).

Table 4 shows that the addition of 0.3% SCGs to cementitious materials reduces the compressive strength to more than 27.31 MPa. The elastic phase of the stress–strain curve of C-3 is steep, and after the maximum compressive stress occurs, strain softening is observed (Figure 4-c).

Table 4. Compressive strength of cementitious materials obtained by adding SCGs with different percentages

Samples	Compressive Strength (MPa)	Average of Compressive Strength (MPa)	Maximum Strain	Error (MPa)
C-1 (1)	39.42	39.48	0.062	±0.77
C-1 (2)	38.71		0.061	
C-1 (3)	40.25		0.061	
C-2 (1)	35.16	35.53	0.056	±0.88
C-2 (2)	36.91		0.058	
C-2 (3)	35.07		0.058	
C-3 (1)	27.31	27.31	0.061	±0.27
C-3 (2)	27.59		0.064	
C-3 (3)	27.03		0.054	

Table 4 shows that C-1 (0.1% SCG addition) provides the highest compressive strength at 39.48 MPa, indicating the positive effect of a small amount of SCGs on the cementitious materials. C-2 (0.2% SCG addition) shows a decrease in compressive strength to 35.53 MPa, indicating that the increase in SCG content begins to inhibit the hydration process. C-3 (0.3% SCG addition) has the lowest compressive strength at 27.31 MPa, indicating that excessive SCGs reduce the mechanical performance, probably due to the interference of organic content with cement hydration. Figure 4 shows the stress–strain curves for the cementitious materials modified with 0.1% SCGs: a relatively steep elastic phase indicates improved strength compared to the control. The stress–strain curve shows a gradual decrease after the peak, indicating that 0.1% SCGs improves the mechanical properties without excessive brittleness. The maximum compressive stress of C-2 is lower than that of C-1 and the strain softening effect becomes more prominent, indicating that excessive SCGs begin to disrupt the cement bond. C-3 (0.3% SCGs) shows a sharp decrease after the peak, indicating brittle failure. The slope of the elastic phase is steeper, but the peak strength is significantly lower, confirming that higher SCG content weakens the mortar structure.

The compressive strength of cementitious materials containing 0.1, 0.2, and 0.3% PSH exhibited significant variation. According to the results, when 0.1% of PSH (P-1) was added to cementitious materials, the compressive strength was 32.52 MPa. The maximum compressive strength of the P-1 sample was over 35.32 MPa and the minimum compressive strength was 30.82 MPa; in this case, the error was ±2.26 MPa. Figure 5-a shows the stress–strain curve of P-1, showing that P-1 has a steep slope. The compressive strength of P-2 was over 35.09 MPa and the maximum and minimum compressive strengths were more than 36.12 and 34.4 MPa, respectively. Table 5 shows that the maximum error for compressive strength was ±0.86. The stress–strain curve of the P-2 specimen shows the error in the elastic phase (Figure 5-b). The compressive strength of the P-3 specimen was over 38.08 MPa and the maximum and minimum compressive strengths were more than 38.83 and 36.98 MPa, respectively. Cementitious materials with the addition of 0.3% PSH exhibited a higher compressive strength compared to the other samples.

Table 5 illustrates P-1 (0.1% PSH addition). The average compressive strength is 32.52 MPa, with a maximum of 35.32 MPa and a minimum of 30.80 MPa. The higher error margin (±2.26 MPa) suggests variability in sample performance. P-2 (0.2% PSH addition) shows a moderate increase in compressive strength to 35.09 MPa, with a lower variability than P-1. The highest recorded value is 36.12 MPa. P-3 (0.3% PSH addition) exhibits the highest compressive strength at 38.08 MPa, with the lowest error margin (±0.92 MPa), indicating consistent mechanical performance. The results suggest that increasing PSH content enhances compressive strength, contrasting with SCG-modified samples where excessive SCGs led to strength reductions. This improvement is likely due to PSH's pozzolanic activity, contributing to additional calcium silicate hydrate (C-S-H) formation, which strengthens the cement matrix.

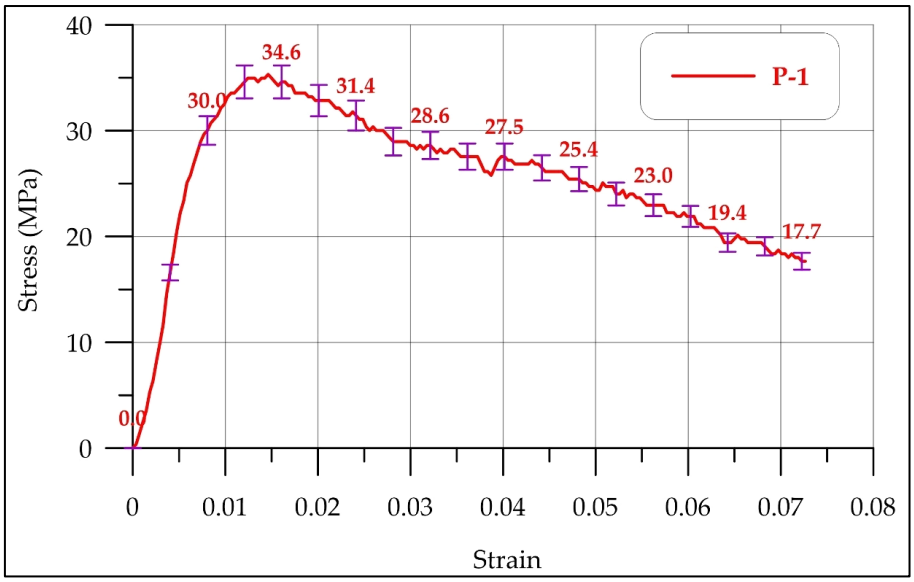

(a)

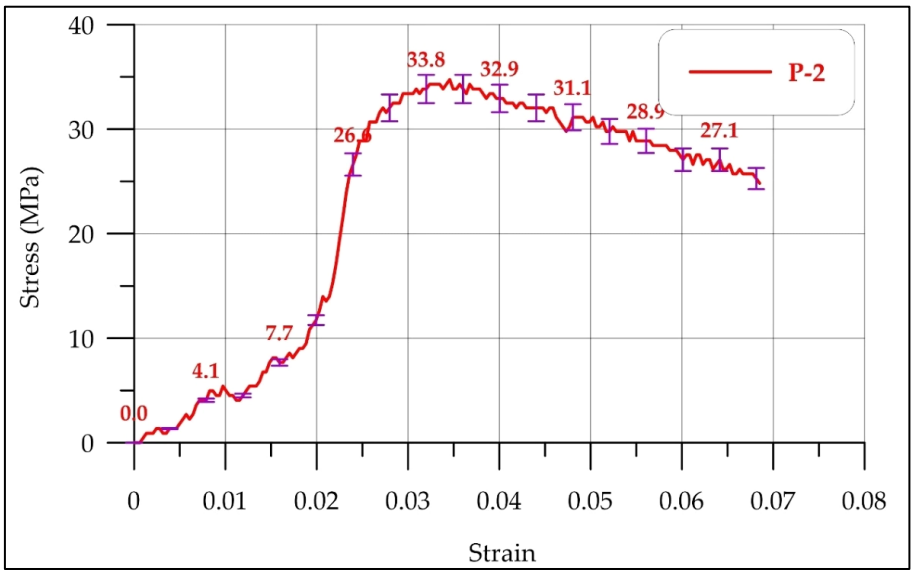

(b)

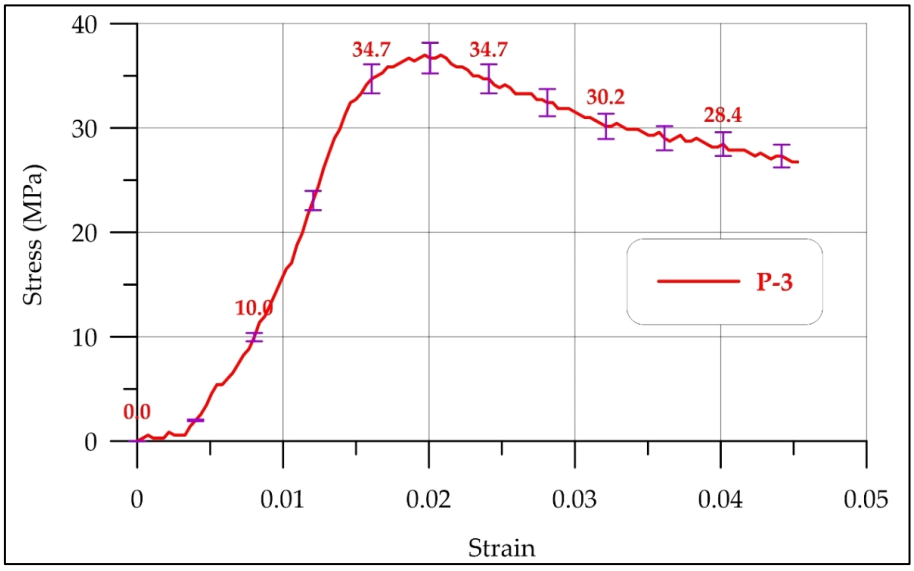

(c)

Figure 5. Compressive strength: (a) P-1 with addition of 0.1% of PSH; (b) P-2 with addition of 0.2% of PSH; (c) P-3 with addition of 0.3% of PSH

Table 5. Compressive strength of cementitious materials obtained by adding PSH with different percentages

Samples	Compressive Strength (MPa)	Average of Compressive Strength (MPa)	Maximum Strain	Error (MPa)
P-1 (1)	35.32		0.073	
P-1 (2)	31.43	32.52	0.065	±1.26
P-1 (3)	30.80		0.063	
P-2 (1)	34.74		0.068	
P-2 (2)	34.4	35.09	0.067	±0.86
P-2 (3)	36.12		0.070	
P-3 (1)	36.98		0.045	
P-3 (2)	38.83	38.08	0.046	±0.92
P-3 (3)	38.44		0.045	

The stress–strain curve in Figure 5-a for P-1 has a steep slope, indicating enhanced load-bearing capacity. However, strain softening occurs post-peak, suggesting that while strength increases, the material remains somewhat brittle. Figure 5-b shows that P-2 (0.2% PSH) displays a higher peak stress than P-1, confirming that a moderate amount of PSH further improves compressive strength. The stress–strain curve also shows a well-defined elastic phase, followed by a gradual decline in load capacity. Figure 5-c shows that P-3 (0.3% PSH) demonstrates the highest compressive strength, with a more uniform stress distribution and delayed failure. The increased ductility compared to lower-PSH samples suggests that PSH acts as a reinforcing agent, reducing brittleness.

3.2. Flexural Strength

The flexural strength was analyzed using the three-point bending test, and the first control sample (C) and the microsilica sample (MS) were evaluated. Table 6 shows the flexural strength of concrete of sample C and M.S., and Table 7 illustrates the flexural strength of cementitious material when SCGs with 0.1, 0.2, and 0.3% percentages were added to cementitious materials.

Table 6. Flexural strength of control sample and control sample with microsilica

Sample	Maximum Flexural Strength (MPa)	Average Maximum Flexural Strength (MPa)	Maximum Displacement (mm)	Force error (kN)
C (1)	2.99		0.47	
C (2)	2.89	2.90	0.46	± 0.047
C (3)	2.83		0.41	
M.S (1)	2.53		0.125	
M.S (2)	2.48	2.48	0.136	± 0.032
M.S(3)	2.43		0.135	

Table 7. Flexural strength of mortar mix obtained by adding SCGs with different percentages

Samples	Maximum Flexural Strength (MPa)	Average of Maximum Flexural Strength (MPa)	Maximum Displacement (mm)	Force error (kN)
C-1 (1)	2.69		0.22	
C-1 (2)	2.66	2.65	0.212	±0.77
C-1 (3)	2.61		0.21	
C-2 (1)	4.52		0.184	
C-2 (2)	4.39	4.45	0.175	±0.029
C-2 (3)	4.43		0.184	
C-3 (1)	3.25		0.109	
C-3 (2)	3.01	3.10	0.098	±0.021
C-3 (3)	3.06		0.097	

According to Table 6, the flexural strength of the control sample (C) was over 2.99 MPa and the minimum was 2.83 MPa; moreover, the average flexural strength was more than 2.90 MPa. The maximum displacement was more than 0.46 mm. The flexural strength of M.S was more than 2.53 MPa and its maximum displacement was between 0.125 and 136 mm. The flexural stress–strain diagram for C and M.S indicates that the C specimen did not exhibit a softening or hardening phase, because of the sudden failure, unlike the case when microsilica was substituted with cement, causing a softening phase in the flexural-displacement mortar mix (Figure 6).

According to Table 6 for the control sample, the average flexural strength is 2.90 MPa, with values ranging from 2.83 to 2.99 MPa. The maximum displacement observed is 0.47 mm, indicating that the control sample exhibits a moderate level of ductility. The force error values suggest minor variations in strength between the tested samples.

For the microsilica sample, the average flexural strength is 2.48 MPa, which is lower than that of the control sample. Maximum displacement values for M.S range from 0.125 to 0.136 mm, significantly lower than those of the control sample, indicating reduced ductility. The error margins are minimal, reflecting consistent test results.

The stress–strain curve for the control Sample (C) shows a more ductile behavior, as shown in Figure 6-a, with a gradual increase in stress followed by a softening phase before failure. No sharp drop is observed, indicating that the control sample undergoes plastic deformation before fracture, making it more resilient under bending forces. Moreover, Figure 6-b shows that the curve for the microsilica sample exhibits a sudden failure mechanism, indicating brittle fracture. The peak stress is lower than that in the control sample, confirming that microsilica decreases flexural strength despite improving compressive strength. The reduction in maximum displacement confirms that MS-modified samples are stiffer but less flexible, making them more prone to sudden breakage.

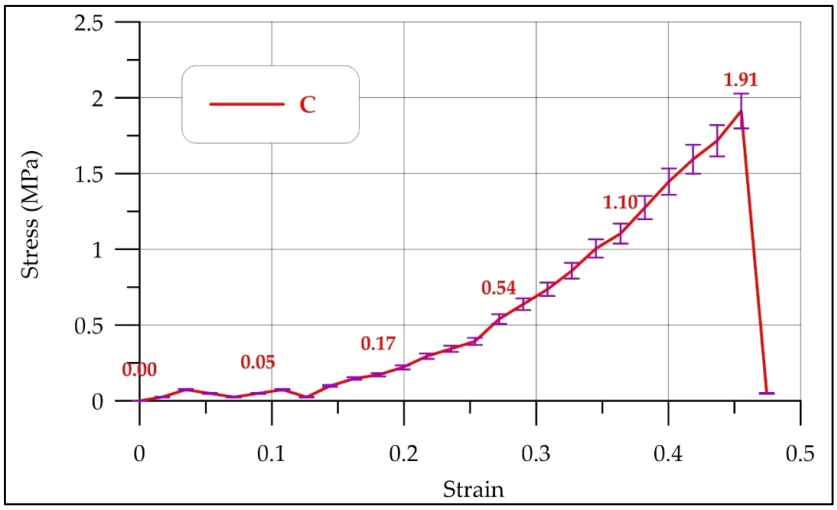

(a)

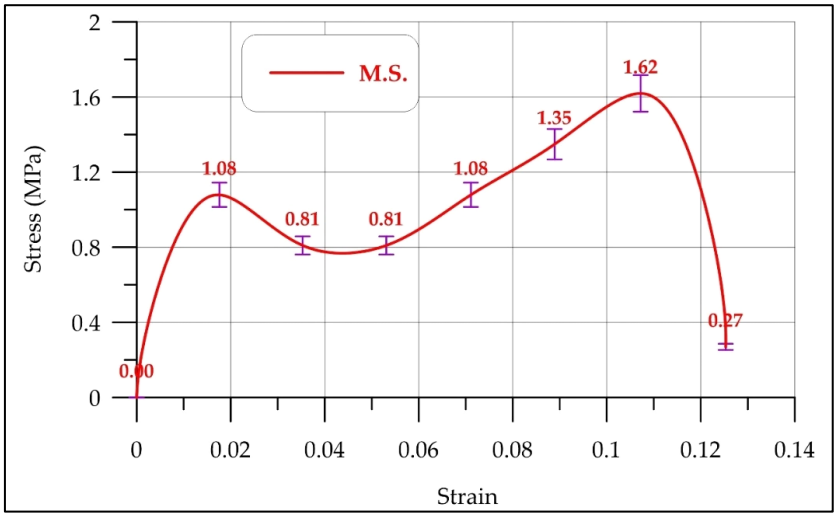

(b)

Figure 6. Flexural strength of cementitious material: (a) control sample (C); (b) control sample with microsilica (M.S)

When SCGs were added in percentages of 0.1, 0.2, and 0.3% to the mortar mix, the flexural strength and flexural displacement changed. The average maximum bending strength for sample C-1 was more than 2.69 MPa, and the maximum displacement was 0.22 mm (Table 7). Figure 7-a shows that the mortar mix had a softening phase after the maximum flexural strength points. The average maximum flexural strength for sample C-2 was over 4.52 MPa and the maximum displacement was 0.184 mm. In addition, the flexural displacement diagram of C-2 shows that this sample had three phases: elastic, inelastic, and plastic. The inelastic phase of P-2 was created after the production of the mortar mix (Figure 7-b). The average maximum bending strength of C-3 was more than 3.10 MPa and the maximum displacement was 0.109 mm. The error of the bending strength for sample C-3 was more than ±0.021. The elastic phase of specimen C-3 is known, and the plastic phase of C-3 of this specimen after yielding shows that the brittleness collapsed (Figure 7-c).

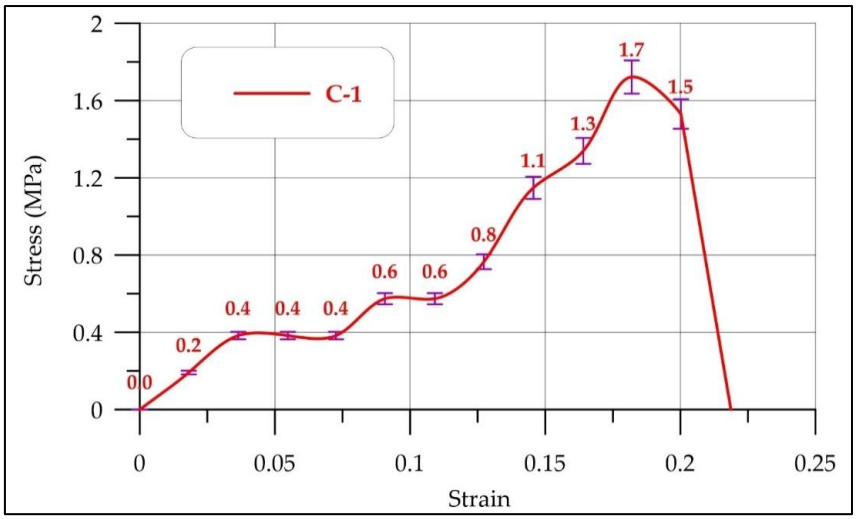

(a)

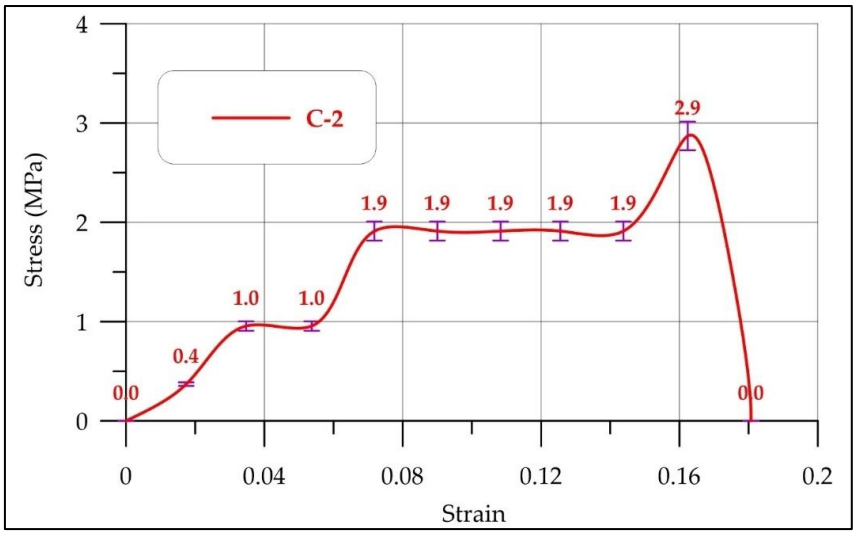

(b)

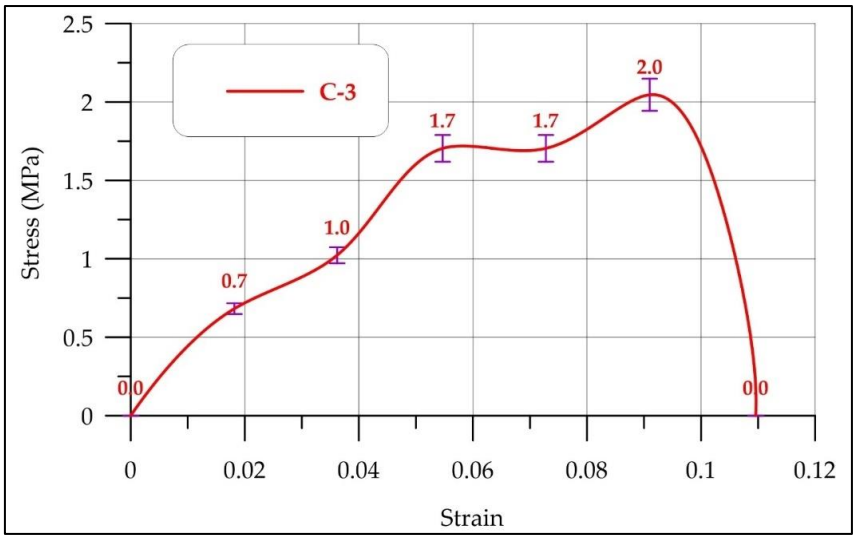

(c)

Figure 7. Flexural strength of (a) C-1 with addition of 0.1% of SCGs, (b) C-2 with addition of 0.2% of SCGs, and (c) C-3 with addition of 0.3% of SCGs

According to Table 7, the average flexural strength of C-1 (0.1% SCG addition) is 2.65 MPa, with individual values ranging from 2.61 to 2.69 MPa. The maximum displacement is 0.22 mm, showing that this sample has some degree of flexibility under bending loads. The C-2 sample shows the highest flexural strength in this sample, reaching an average of 4.45 MPa. The maximum displacement is 0.184 mm, indicating that the material maintains good structural integrity

under bending forces. The stress–strain behavior shows well-defined elastic, inelastic, and plastic phases, demonstrating that SCGs at 0.2% contribute to increased flexural strength and ductility. Moreover, the C-3 sample illustrates that the flexural strength drops to 3.10 MPa, lower than that of C-2 but still higher than that of the control sample. The maximum displacement is 0.109 mm, indicating that the material becomes stiffer and more brittle at this higher SCG concentration. The force error for C-3 is ±0.021 kN, showing minor variations between test samples.

According to Figure 7, the stress–strain curve of C-1 shows a moderate increase in stress followed by a gradual softening phase. The material exhibits some degree of plastic deformation before failure, indicating improved flexural strength over the control sample. C-2 shows the highest peak flexural strength among all SCG samples. The stress–strain curve reveals three distinct phases, elastic, inelastic, and plastic, confirming enhanced mechanical performance. The ductility of this sample is higher, making it less prone to sudden failure under bending loads. For C-3, the stress–strain curve exhibits a steep elastic phase followed by a sharp drop, indicating brittle failure. The material becomes more rigid with increasing SCG content, reducing flexural capacity beyond 0.2% SCGs. The plastic phase is almost absent, confirming that higher SCG percentages negatively affect flexural performance.

Adding PSH in percentages of 0.1, 0.2, and 0.3% to the mortar mix had a significant effect on the mechanical properties of the mortar mix. Table 8 illustrates that when 0.1% of PSH was added to cementitious material, the flexural strength improved to more than 6.11 MPa, while the maximum displacement was 0.16 mm. The flexural strength–displacement diagram of P-1 illustrates that after the yielding of the sample, mortar mix ductility continued until an ultimate point (Figure 8-a). The flexural strength of P-2 was over 3.8 MPa and the maximum displacement was 0.31 mm. The flexural strength–displacement curve shows that the maximum phase of cementitious material with the addition of 0.2% of PSH had elastic and inelastic phases before the point of ultimate strength (Figure 8-b). The results of P-3 show when 0.3% of PSH was added to the mortar mix, the maximum flexural strength was 3.93 MPa, while the maximum displacement was 0.93 mm (Figure 8-c).

Table 8. Flexural strength of mortar mix obtained by adding PSH with different percentages

Samples	Maximum Flexural Strength (MPa)	Average of Maximum Flexural Strength (MPa)	Maximum Displacement (mm)	Force error (kN)
P-1 (1)	6.06	6.02	0.14	±0.22
P-1 (2)	5.89		0.15	
P-1 (3)	6.11		0.16	
P-2 (1)	3.81	3.41	0.31	±0.25
P-2 (2)	3.39		0.29	
P-2 (3)	3.05		0.31	
P-3 (1)	3.76	3.77	0.91	±0.094
P-3 (2)	3.64		0.9	
P-3 (3)	3.93		0.93	

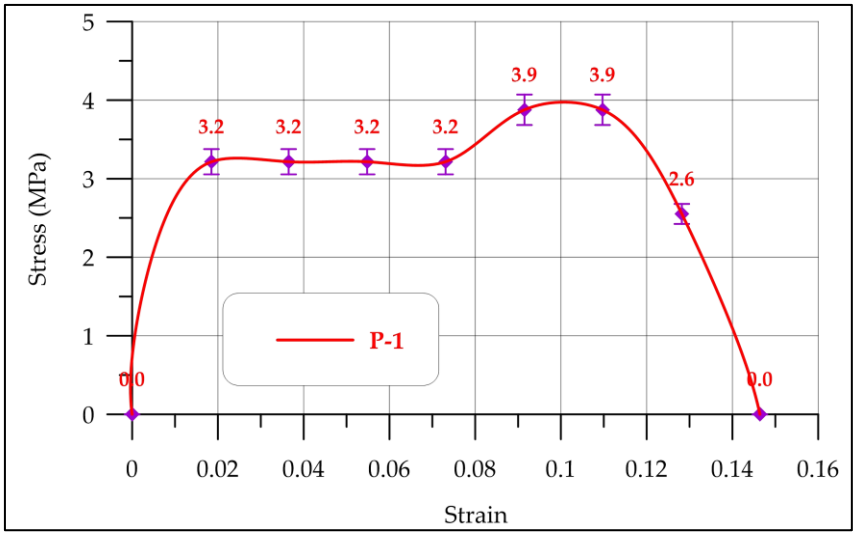

(a)

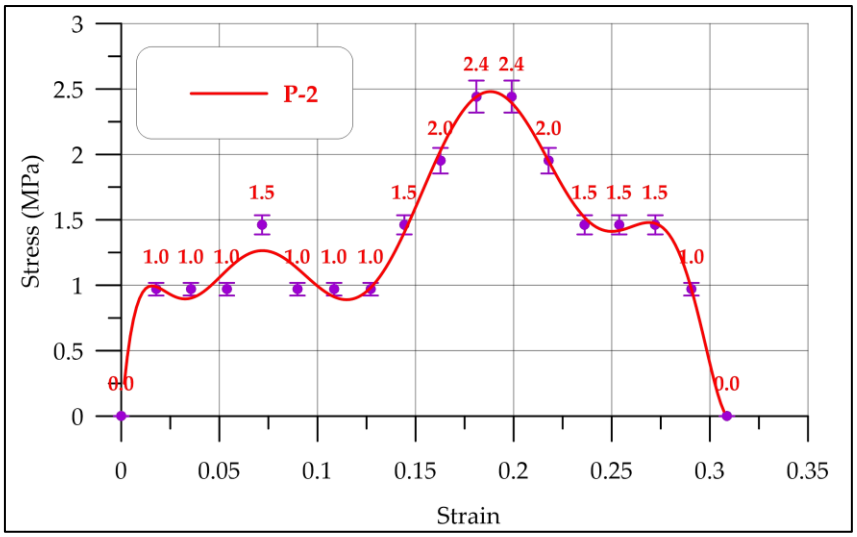

(b)

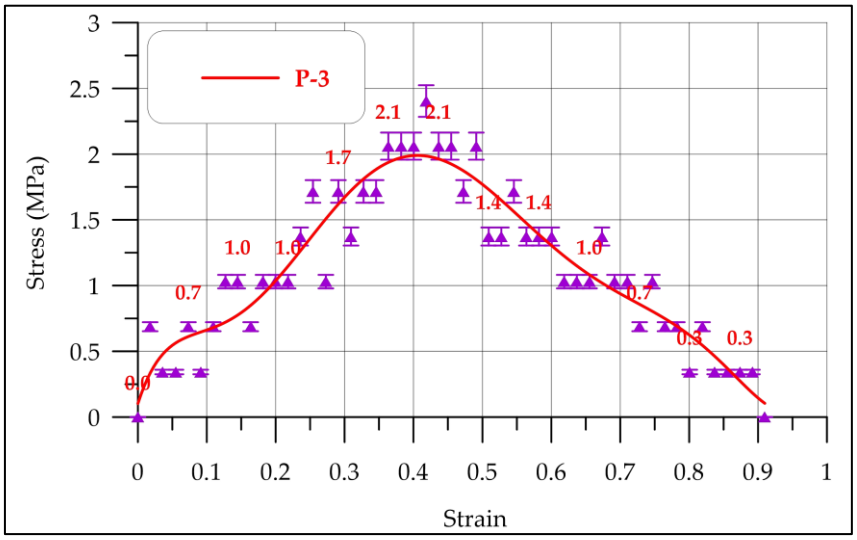

(c)

Figure 8. Flexural strength of (a) P-1 with addition of 0.1% of PSH, (b) P-2 with addition of 0.2% of PSH, and (c) P-3 with addition of 0.3% of PSH

According to Table 8, the average flexural strength is 6.02 MPa, with individual values ranging from 5.89 to 6.11 MPa. The maximum displacement is 0.16 mm, showing that this mix provides improved load-bearing capacity while maintaining some flexibility (P-1). P-2 shows that the flexural strength decreases to 3.41 MPa, significantly lower than that of P-1. The maximum displacement increases to 0.31 mm, suggesting that, while the material becomes more flexible, it loses some strength. The higher displacement values indicate better ductility compared to the control and SCG-modified samples. Finally, P-3 illustrates that the average flexural strength is 3.77 MPa, slightly higher than that of P-2 but still lower than that of P-1. The maximum displacement reaches 0.93 mm, confirming that this sample is the most ductile among the PSH-modified mixes. The force error is ±0.094 kN, reflecting minimal variations between test samples.

3.3. Fracture Mode Analysis

This section presents the examination of the fracture model of the mortar mix with and without M.S, SCGs, and PSH. In this regard, the first cube fracture model under compressive load and subsequent flexural strength prisms was investigated.

Figure 9 illustrates the fracture model of the mortar mix under compression loading. According to Figure 9, the control sample and the mortar mix with the addition of microsilica and SCGs were brittle, as shown by the fracture model in Figures 9-b to 9-d. By contrast, when PSH was added to the mortar mix, the fracture model was soft, as shown in Figures 9-f to 9-h. These brittle and tough fractures were due to the fact that adding SCGs as a filler improved the chemical properties of concrete, while the addition of PSH acted as a fiber and prevented the separation of the cement matrix.

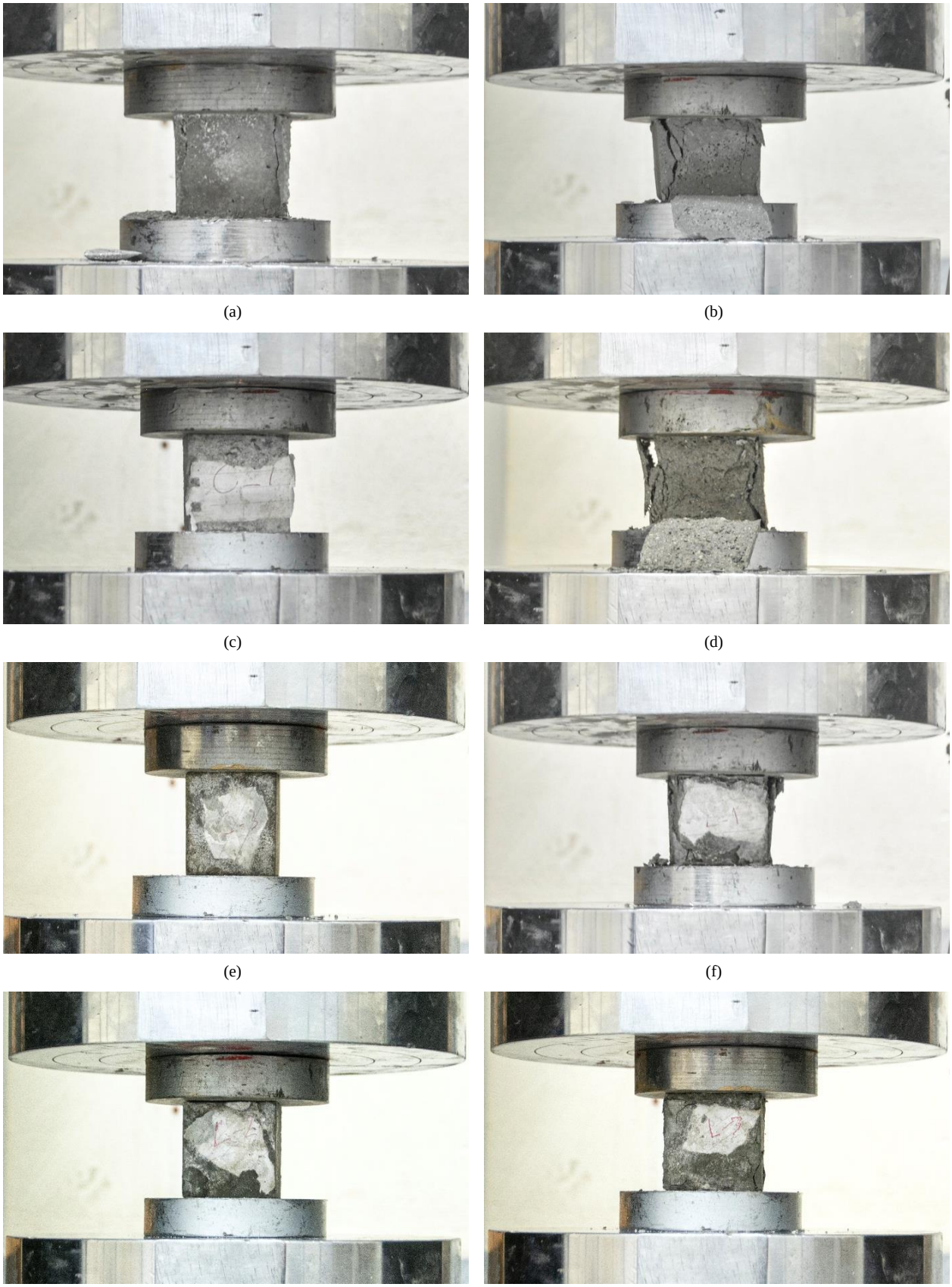

(a) (b)

(c) (d)

(e) (f)

(g) (h)

Figure 9. Fracture modes of compressive strength: (a) C, (b) M.S, (c) C-1, (d) C-2 (e) C-3, (f) P-1, (g) P-2, and (h) P-3

The prism fracture model shows that most fractured samples start with a crack and continue until the fracture prism is complete. In Figure 10, a small, almost horizontal crack is evident under the prism. In fact, this figure shows the moment before the specimens fractured. In this way, most of the prism fractures were brittle and sudden.

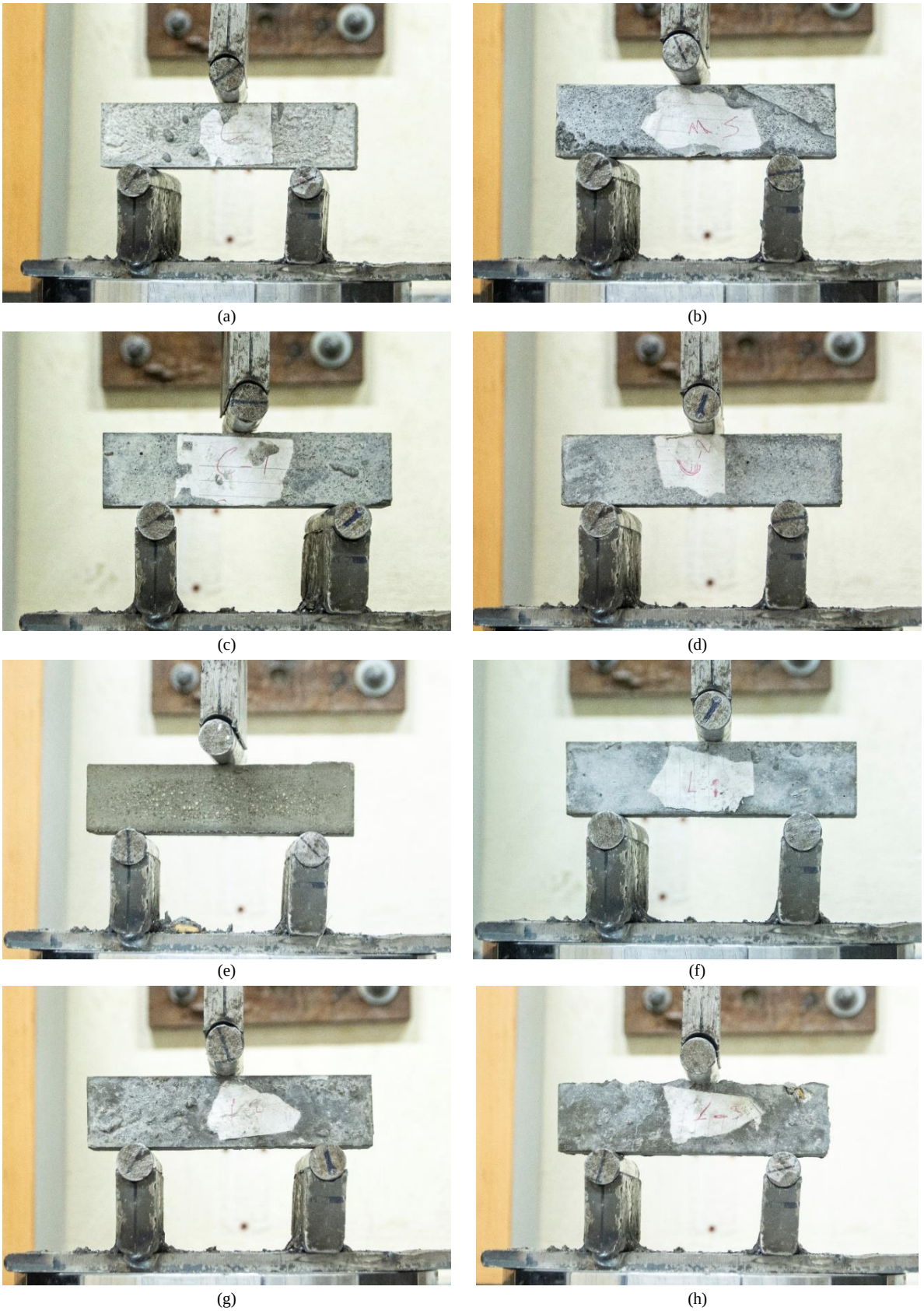

Figure 10. Fracture models of flexural strength: (a) C; (b) M.S; (c) C-1; (d) C-2; (e) C-3; (f) P-1; (g) P-2; (h) P-3

3.4. Scanning Electron Microscope (SEM) and Energy Dispersive X-Ray (EDX) Analysis

Due to the absence of aggregates and the replacement of marble dust, the cement matrix consists of cement and marble dust in Figure 11-a. The voids are clear in Figure 11-b because of insufficient shaking and a lack of filler. As shown in Figure 11-a and Table 9, the effect of PSH on the C-S-H and calcium aluminate hydrate (C-A-H) phases indicates that Si and Al from PSH combine with Ca $(OH)_2$ released during cement hydration, leading to the formation of additional C-S-H and calcium aluminate hydrate (C-A-H) phases. This reaction increases compressive strength,

reduces porosity, and improves durability, while SCGs introduce organic matter and carbon-based particles into the cement matrix. These organic compounds can coat cement grains, interfere with ion diffusion, delay the hydration of tricalcium silicate (C_3S) and dicalcium silicate (C_2S), and inhibit the formation of C-S-H. Yee et al. [38] found that SCGs contain more than one-third oxygen and two-thirds carbon, improving the oxygen in C-3. The EDX analysis results were related to the rich source of SCGs from oxygen. Figure 11-c shows the C-S-H crystals. Lee et al. [39] also added SCGs to concrete and found similar SEM images using a similar crystal; however, in the current study, the amount of crystal is greater due to the use of microsilica.

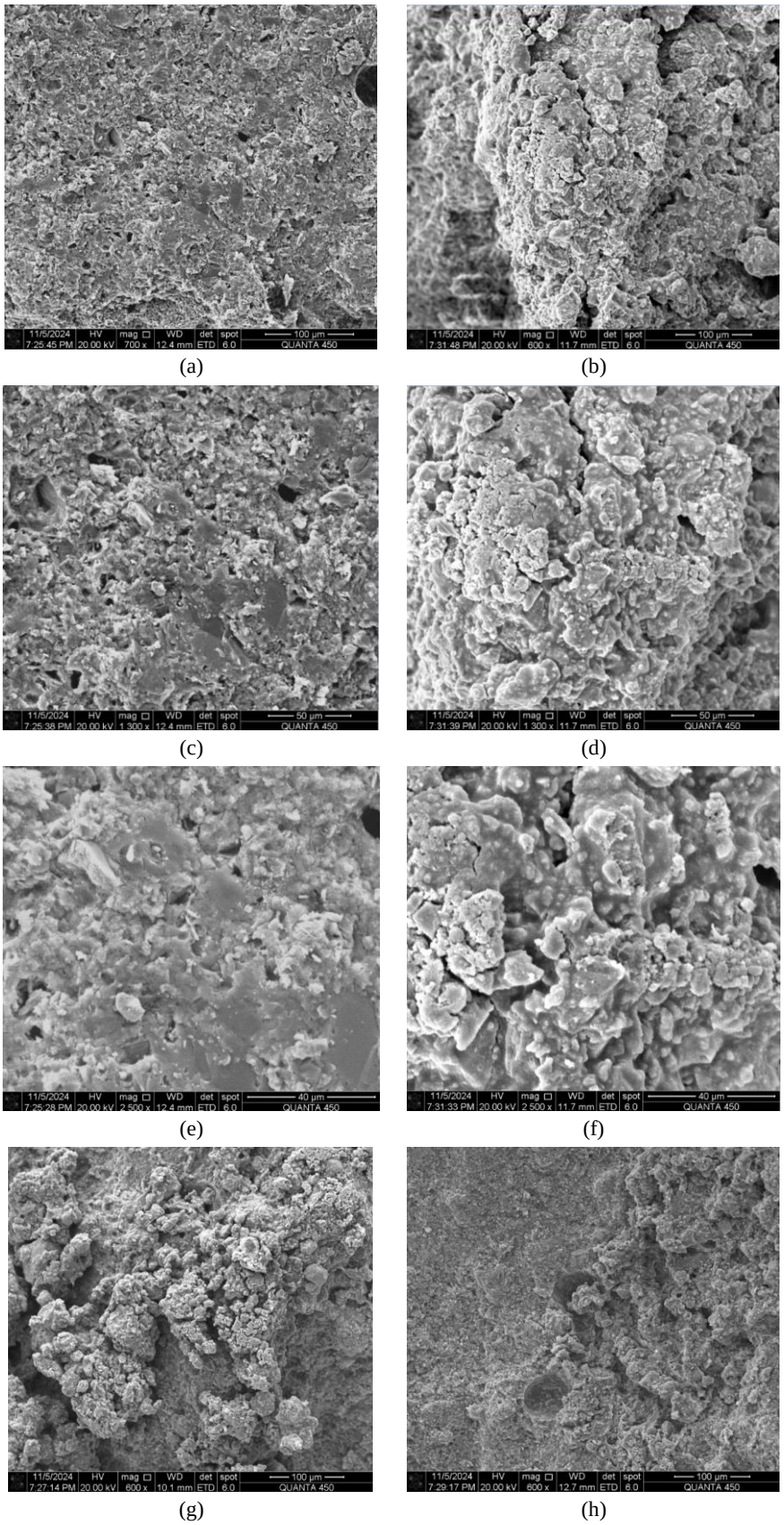

(a) (b)

(c) (d)

(e) (f)

(g) (h)

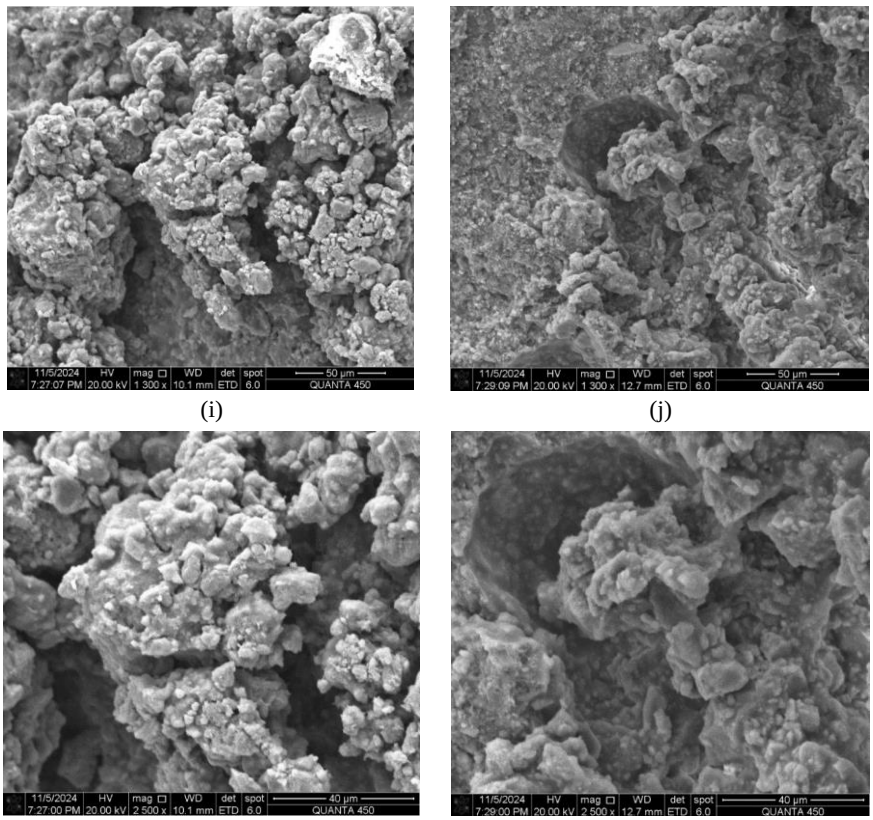

Figure 11. SEM pictures. Control sample (C): (a) 700×, (c) 1300×, and (e) 2500×; microsilica sample (M.S): (b) 600×, (d) 1300×, and (f) 2500×; C-3: (g) 600×, (i) 1300×, and (k) 2500×; and P-3: (h) 600×, (j) 1300×, and (l) 2500×

Adding PSH was the cause of increasing Si to more than 6.53%, Al to more than 0.61%, and added sodium (Na) to more than 0.07% in the chemical composition of P-3. In any case, adding 0.3% of PSH improved C-S-H because of Si and Al in the cement matrix (Table 9, Figure 12-d). In addition, crystals were clear in the P-3 samples, although when SCGs were added as a filler, PSH was used as a fiber agent and improved the C-S-H process (Figure 11-d).

Table 9. EDX results of C, M.S, C-3, and P-3 samples

Sample\Elements	C	O	Mg	Al	Si	K	Ca	Fe	MO	Na
C (norm Wt%)	10.80	48.92	1.38	0.39	1.79	1.25	34.80	0.66	-	-
M.S (norm Wt%)	7.45	48.75	0.95	0.59	6.12	1.09	32.75	0.72	1.58	-
C-3 (norm Wt%)	13.00	51.60	0.70	0.40	5.05	0.91	27.40	0.20	0.74	-
P-3 (norm Wt%)	9.33	49.74	0.96	0.61	6.53	1.04	29.76	0.54	0.54	0.07

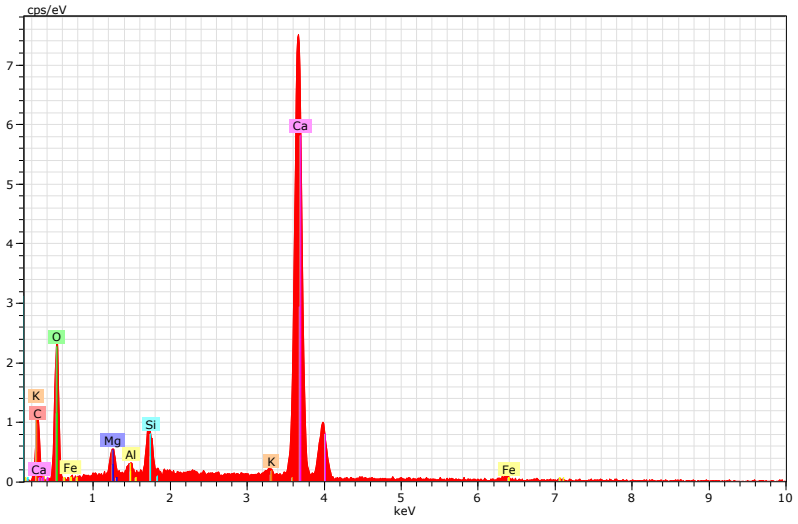

(a)

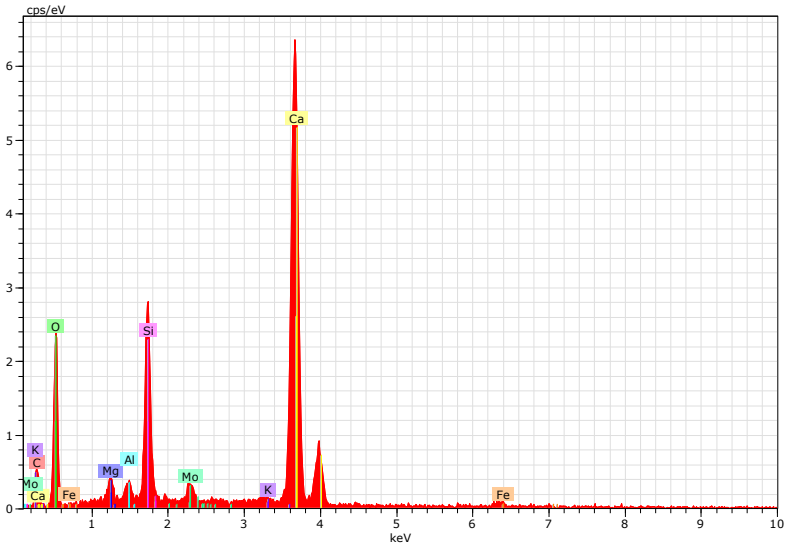

(b)

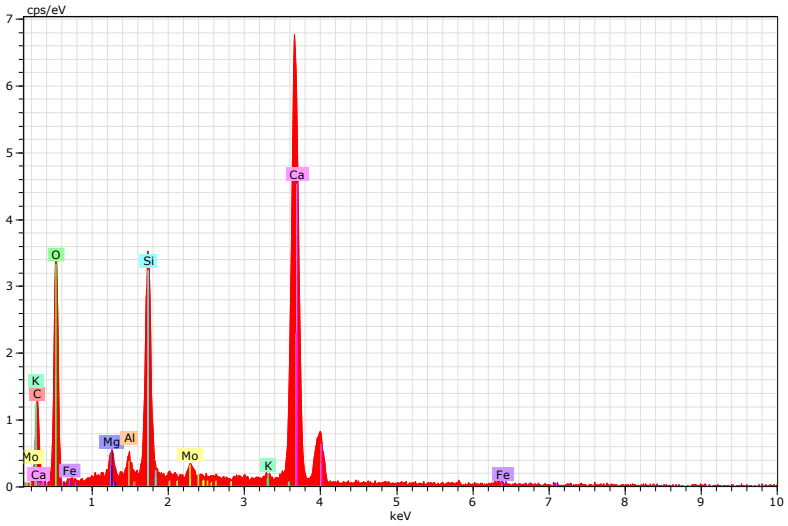

(c)

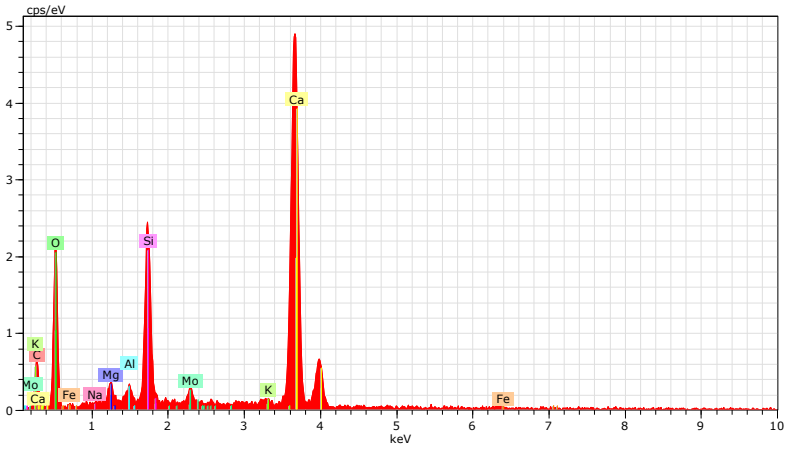

(d)

Figure 12. EDX: (a) control sample (C), (b) microsilica sample (M.S), (c) C-3, and (d) P-3

4. Discussion

According to the results, adding SCGs and PSH influenced the mechanical properties, fracture model, and chemical composition of the cement matrix. Figure 13 illustrates the compressive strength and flexural strength of all the samples.

The maximum compressive strength corresponded with C-1 with 39.48 MPa, followed by P-3 with 38.09 MPa. Considering Figure 13-a, the compressive strength of C-1 and P-3 improved more than 18.1 and 14% rather than C (control sample). The compressive strength trend of the mortar mix grew when PSH was added, while this trend declined

when SCGs were added. Figure 13-b shows that when SCGs and PSH were added to the mortar mix, the flexural strengths of C-2 and P-1 improved to the maximum. However, adding PSH and SCGs showed good performance, as well as adding PSH to cementitious materials.

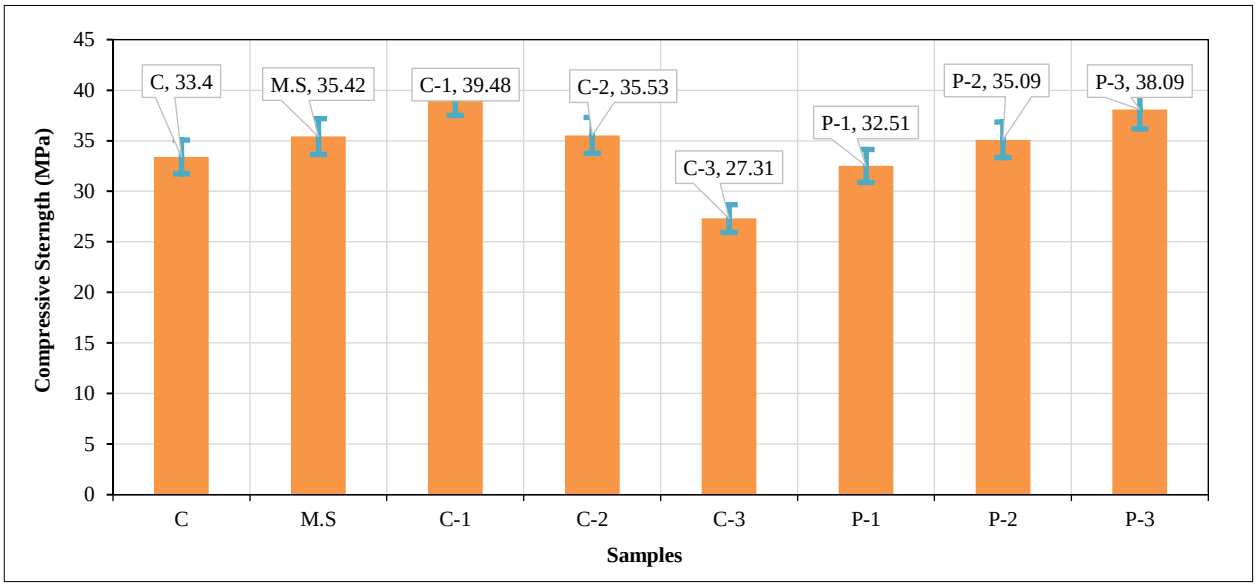

(a)

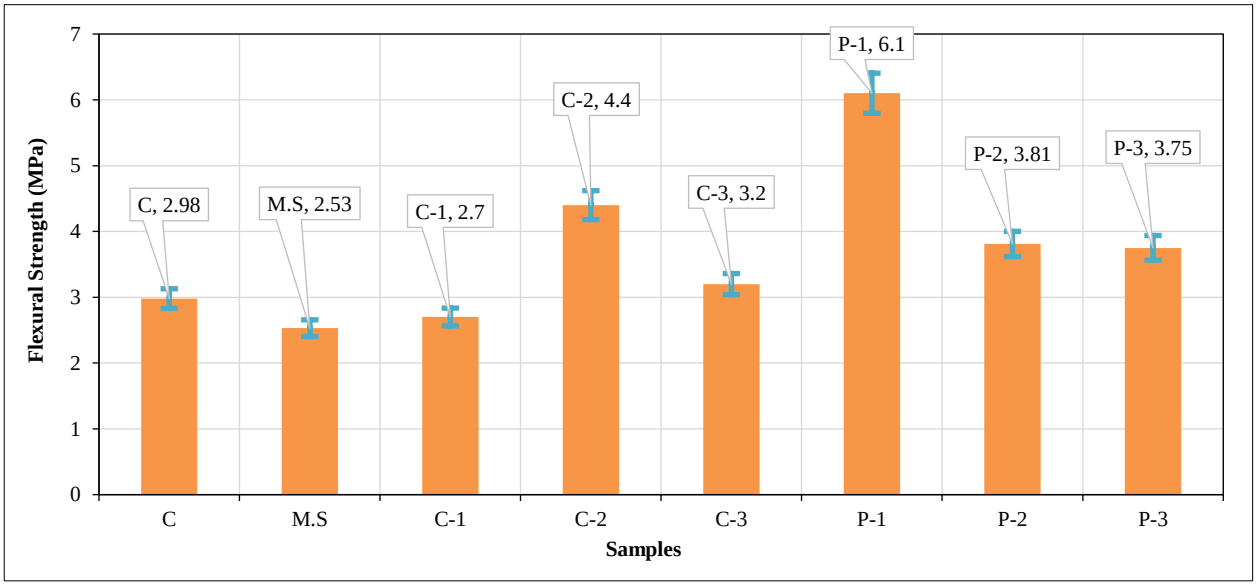

(b)

Figure 13. Mechanical properties of mortar mix: (a) compressive and (b) flexural strengths

Other studies have shown different results. For example, Gwarah et al. [40] added different percentages of Bambara groundnut shell ash to concrete in percentages from 0 to 50%. They found that by increasing the Bambara groundnut shell ash, compressive strength was significantly reduced. Their results showed that when 10% of Bambara groundnut shell ash was added to concrete, the compressive strength reduced more than 22%, and when 50% was added, the compressive strength decreased more than 84%. Unlike Ikumapayi et al.'s [41] results, adding PSH to the mortar mix in the current study improved the compressive strength by more than 14%. In another study, the researchers added 8% of groundnut shell ash to the concrete and found that the compressive strength was slightly increased after 28 days of curing [42]. For instance, samples at 28 days of curing had a compressive strength of 21.34 MPa. However, extending the curing time to over 56 days resulted in a 10% increase in the compressive strength of concrete samples when adding extra groundnut shell ash [42].

This study, like previous research, shows that adding SCGs to concrete lowers its compressive strength. A previous study shows that when SCGs are added to cement ventilation blocks, compressive strength decreases. Thus, by increasing the amount of salt added, the compressive strength of the concrete decreases [43]. Other studies have attempted to combine grinding powder (OS.P) or crushed-granular (OS.G) forms with SCGs with a special ratio to find the best composite. Le et al. [44] showed that when the ratio of OS.P/SCGs increased, the compressive strength improved too, while according to other studies and the current study, when SCGs increased, the compressive strength increased.

Overall, adding SCGs and PSH to the mortar mix is comparable. Considering the results, SCGs acted as a filler; moreover, it helped improve the compressive strength when 0.1% was added to the mortar mix. On the other hand, when PSH was added to the mortar mix, compressive strength increased. It is clear that adding PSH to the mortar mix can improve compressive and flexural strengths. Finally, this study proves the initial hypotheses: adding SCGs has the greatest impact on the chemical properties and on improving the mechanical properties, while adding PSH to the mortar mix increases the compressive and flexural strengths due to the nature of PSH and the geometry, such as fibers. Moreover, this study proves that using cementitious material is sustainable due to adding PSH, SCGs, and marble dust.

PSH has better mechanical properties than SCGs. PSH contains a high percentage of silica (SiO_2) and alumina (Al_2O_3), which are reactive pozzolanic components. These elements react with the $Ca(OH)_2$ released during hydration to form a C-S-H adduct gel that improves compressive and flexural strengths. By contrast, SCGs lack significant amounts of Si and Al, making it ineffective in promoting hydration and secondary cementitious reactions. PSH has a fibrous morphology that acts as a micro-reinforcement in the cement matrix. The fibrous nature of PSH helps distribute stress more effectively, reduce crack propagation, and improve ductility. SCGs, on the other hand, act primarily as a filler, meaning it modifies the pore structure but does not contribute to tensile strength or crack bridging. PSH particles intertwine with cement hydrates and strengthen the bond between particles, resulting in a denser and more cohesive microstructure. This cohesive effect improves mechanical performance by reducing weak spots in the mortar mix. SCGs, due to their fine and amorphous nature, fill voids but does not create the same interlocking effect and is less effective in increasing strength. The failure mode analysis in this study showed that PSH-modified samples showed more gradual failure patterns, while SCG-modified samples at higher concentrations had brittle failures. This confirms that PSH improves toughness and energy absorption capacity, making it a better structural additive. PSH helps reduce porosity by actively participating in hydration reactions and filling voids with C-S-H gel. SCGs, when added in excess, increase porosity due to their organic nature, which can hinder hydration and create weak zones.

According to this investigation, SCGs and PSH were chosen for different reasons. The combined effect of SCGs and PSH not only enhances the mechanical properties of the mortar but also contributes to its long-term durability. The microstructural analysis (SEM and EDX) confirmed that PSH actively participates in the hydration process, increasing the formation of calcium silicate hydrate (C-S-H), which is responsible for strength development. Additionally, PSH introduces alumina and silica compounds, further promoting pozzolanic activity, thereby improving compressive and flexural strengths.

On the other hand, SCGs, acting as a filler, refine the pore structure of the mortar mix. The porosity reduction observed in SCG-modified samples is attributed to the carbon-rich composition of coffee grounds, which fills voids in the cement matrix. However, excessive SCG content (0.3%) was found to slow down hydration reactions, leading to a decline in compressive strength. This effect highlights the importance of optimal dosage when incorporating SCGs into cementitious materials. Another critical advantage of using SCGs and PSH over other waste materials is their compatibility with microsilica. The addition of microsilica (SiO_2) was observed to enhance the mechanical performance of the mortar by further refining the cement matrix. However, without PSH, microsilica alone did not provide significant improvements in flexural strength, as brittle failure was still observed. The synergistic effect of PSH and microsilica reduced this brittleness, ensuring a more ductile fracture behavior. Moreover, thermal resistance and chemical durability are important factors in assessing the feasibility of SCGs and PSH in construction applications. Unlike other organic additives such as carrot extract or humid acid, which primarily impact hydration kinetics, SCGs and PSH contribute directly to structural reinforcement. The presence of lignin in PSH further enhances its thermal resistance, making it a more robust additive compared to traditional agricultural waste materials.

The use of marble dust in combination with SCGs and PSH further contributes to the sustainability of the mix by replacing a portion of cement or fine aggregates, reducing the overall carbon footprint of the material. This approach aligns with modern trends in eco-friendly construction, where minimizing cement consumption while maintaining structural integrity is a key objective. Ultimately, the findings of this study demonstrate that SCGs and PSH offer a unique balance between strength enhancement, sustainability, and durability, making them superior alternatives to many conventional bio-waste additives. The optimized incorporation of these materials into cementitious mixes can pave the way for cost-effective and environmentally friendly construction solutions.

By keeping marble dust as a constant additive, this study ensured that the observed changes in mechanical and chemical properties could be directly attributed to the different ratios of SCGs and PSH rather than fluctuations in the base materials. This methodological decision also allowed for a more accurate comparison of how organic waste additives interact with the cement matrix while taking advantage of the void-filling properties of marble dust.

Furthermore, the interaction between marble dust, PSH, and SCGs showed distinct patterns in hydration kinetics and microstructural development. While marble dust acts primarily as a passive filler, PSH actively participates in the

pozzolanic reaction, leading to the formation of additional C-S-H gels that contribute to the development of long-term strength. The higher silica and alumina contents in PSH facilitated stronger bonding in the cement matrix, which was reflected in the increased flexural and compressive strengths of PSH-modified specimens.

On the contrary, SCGs affected the hydration process differently. At low concentrations (0.1%), it contributed to a denser microstructure, reduced porosity, and increased strength at early ages. However, at higher doses (0.3%), SCGs interfered with hydration, slowing down the formation of C-S-H, which led to a decrease in compressive strength. This suggests that the role of SCGs is more microstructural than chemical, as it does not actively participate in pozzolanic reactions like PSH, but instead modifies the pore distribution and density.

The range of 0.1 to 0.3% was strategically chosen to maximize the benefits while minimizing the disadvantages. Lower doses produce minimal measurable effects, while higher doses can compromise workability, hydration, and structural performance. The results of this study reinforce that an optimal ratio of SCGs and PSH can effectively enhance the mortar's properties, but their use must be carefully controlled to avoid negative trade-offs. The findings of this study confirm that controlling the SCG and PSH doses within the selected range (0.1–0.3%) results in measurable improvements in additional mechanical properties associated with the additional materials. The results indicate that each dose level has distinct effects, confirming the necessity of a controlled experimental approach.

5. Conclusions

A sustainable cement material, incorporating cement, marble dust, microsilica, peanut shell, spent coffee grounds, water, and superplasticizer, was investigated in this study. To compare mechanical (compressive and flexural strengths) and microstructure properties, SEM and EDX analyses were performed. According to results, adding microsilica can improve the compressive strength while decreasing the flexural strength. The most important effect of the addition of microsilica is the formation process of C-S-H in order to increase the compressive strength, although the excessive addition of SCGs has a negative effect on the effectiveness of this process, while the increase in the addition of PSH to the mortar mix has a positive effect on this process. Accordingly, the following points summarize this paper:

- The inclusion of microsilica in the mortar mixture increases the compressive strength by more than 35.42 MPa compared to 33.4 MPa of the control sample.
- Most of the stress–strain curves and flexural load–displacement graphs have strain softening characteristics. When PSH is added to the cement material, strain softening changes to strain hardening, especially in flexural loading.
- Adding PSH to cement material produces a greater effect than adding SCGs, because PSH exhibits fibrous properties, whereas SCGs function as a filler.
- Because PSH has a fibrous structure, samples with PSH addition fractured gradually, unlike the other samples, which fractured suddenly.
- According to the results, adding 0.3% SCG decreased the compressive strength and reduced the effect of C-S-H processes, while adding 0.3% PSH increased the compressive strength and improved the effect of C-S-H processes.

6. Declarations

6.1. Author Contributions

Conceptualization, M.H. and K.M.; methodology, S.A.S.; software, E.M.S.; validation, M.H., K.M., and A.N.B.; formal analysis, A.N.B.; investigation, A.N.B., M.H., K.M., S.A.S., and E.M.S.; resources, M.H.; data curation, K.M.; writing—original draft preparation, A.N.B., M.H., S.A.S., and E.M.S.; writing—review and editing, A.N.B., M.H., S.A.S., and E.M.S.; visualization, M.H. and K.M.; supervision, A.N.B.; project administration, A.N.B.; funding acquisition, E.M.S. All authors have read and agreed to the published version of the manuscript.

6.2. Data Availability Statement

The data presented in this study are available in the article.

6.3. Funding and Acknowledgments

The authors would like to acknowledge the administration of Don State Technical University for the resources and financial support.

6.4. Conflicts of Interest

The authors declare no conflict of interest.

7. References

[1] Antipas, I. R., & Dyachenko, A. G. (2022). Using the Finite Element Method to Simulate a Carbon Fiber Reinforced Polymer Pressure Vessel. Advanced Engineering Research, 22(2), 107–115. doi:10.23947/2687-1653-2022-22-2-107-115.

[2] Morgun, V. N. (2023). About Dynamics of Improving the Foam Concrete Technological and Operational Properties upon Disperse Reinforcement with Polypropylene Fibers. Modern Trends in Construction, Urban and Territorial Planning, 2(4), 69–76. doi:10.23947/2949-1835-2023-2-4-69-76.

[3] Chiadighikaobi, P. C., Hasanzadeh, A., Hematibahar, M., Kharun, M., Mousavi, M. S., Stashevskaya, N. A., & Adegoke, M. A. (2024). Evaluation of the mechanical behavior of high-performance concrete (HPC) reinforced with 3D-Printed trusses. Results in Engineering, 22. doi:10.1016/j.rineng.2024.102058.

[4] Chiadighikaobi, P. C., Hematibahar, M., Kharun, M., Stashevskaya, N. A., & Camara, K. (2024). Predicting mechanical properties of self-healing concrete with Trichoderma Reesei Fungus using machine learning. Cogent Engineering, 11(1), 2307193. doi:10.1080/23311916.2024.2307193.

[5] Hematibahar, M., Hasanzadeh, A., Kharun, M., Beskopylny, A. N., Stel'makh, S. A., & Shcherban', E. M. (2024). The Influence of Three-Dimensionally Printed Polymer Materials as Trusses and Shell Structures on the Mechanical Properties and Load-Bearing Capacity of Reinforced Concrete. Materials, 17(14), 3413. doi:10.3390/ma17143413.

[6] Stel'makh, S. A., Beskopylny, A. N., Shcherban', E. M., Mavzolevskii, D. V., Drukarenko, S. P., Chernil'nik, A. A., Elshaeva, D. M., & Shilov, A. A. (2024). Influence of corn cob ash additive on the structure and properties of cement concrete. Construction Materials and Products, 7(3), 2. doi:10.58224/2618-7183-2024-7-3-2.

[7] Pan, J., Feng, K., Chen, W., Xing, W., & Wang, Y. (2023). Carrot extract as bio-admixture for performance enhancement of tunnel lining concrete. Journal of Building Engineering, 75, 107036. doi:10.1016/j.jobe.2023.107036.

[8] Hakeem, I. Y., Amin, M., Zeyad, A. M., Tayeh, B. A., Maglad, A. M., & Agwa, I. S. (2022). Effects of nano sized sesame stalk and rice straw ashes on high-strength concrete properties. Journal of Cleaner Production, 370, 133542. doi:10.1016/j.jclepro.2022.133542.

[9] Shao, L., Ding, Z., Wang, S., Pan, K., & Hu, C. (2023). Effect of Organic Matter Components on the Mechanical Properties of Cemented Soil. Materials, 16(17), 5889. doi:10.3390/ma16175889.

[10] D'Eusanio, V., Bertacchini, L., Marchetti, A., Mariani, M., Pastorelli, S., Silvestri, M., & Tassi, L. (2023, June). Rosaceae Nut-Shells as Sustainable Aggregate for Potential Use in Non-Structural Lightweight Concrete. Waste, 1(2), 549-568. doi:10.3390/waste1020033.

[11] Liu, D., Zhang, B., Yang, Y., Xu, W., Ding, Y., & Xia, Z. (2018). Effect of Organic Material Type and Proportion on the Physical and Mechanical Properties of Vegetation-Concrete. Advances in Materials Science and Engineering, 2018. doi:10.1155/2018/3608750.

[12] Siddique, R. (2012). Utilization of wood ash in concrete manufacturing. Resources, Conservation and Recycling, 67, 27–33. doi:10.1016/j.resconrec.2012.07.004.

[13] Traore, Y. B., Messan, A., Hannawi, K., Gerard, J., Prince, W., & Tsobnang, F. (2018). Effect of oil palm shell treatment on the physical and mechanical properties of lightweight concrete. Construction and Building Materials, 161, 452–460. doi:10.1016/j.conbuildmat.2017.11.155.

[14] Zheng, W., Phoungthong, K., Lü, F., Shao, L. M., & He, P. J. (2013). Evaluation of a classification method for biodegradable solid wastes using anaerobic degradation parameters. Waste Management, 33(12), 2632–2640. doi:10.1016/j.wasman.2013.08.015.

[15] Bhatt, S. M., & Shilpa, S. (2014). Bioethanol production from economical agro waste (groundnut shell) in SSF mode. Research Journal of Pharmaceutical, Biological and Chemical Sciences, 5(6), 1210–1218.

[16] Duc, P. A., Dharanipriya, P., Velmurugan, B. K., & Shanmugavadivu, M. (2019). Groundnut shell -a beneficial bio-waste. Biocatalysis and Agricultural Biotechnology, 20, 101206. doi:10.1016/j.bcab.2019.101206.

[17] Ding, M., Satija, A., Bhupathiraju, S. N., Hu, Y., Sun, Q., Han, J., Lopez-Garcia, E., Willett, W., Van Dam, R. M., & Hu, F. B. (2015). Association of coffee consumption with total and cause-specific mortality in 3 large prospective cohorts. Circulation, 132(24), 2305–2315. doi:10.1161/CIRCULATIONAHA.115.017341.

[18] Murthy, P. S., & Naidu, M. M. (2012). Recovery of Phenolic Antioxidants and Functional Compounds from Coffee Industry By-Products. Food and Bioprocess Technology, 5(3), 897–903. doi:10.1007/s11947-010-0363-z.

[19] Roychand, R., Kilmartin-Lynch, S., Saberian, M., Li, J., Zhang, G., & Li, C. Q. (2023). Transforming spent coffee grounds into a valuable resource for the enhancement of concrete strength. Journal of Cleaner Production, 419, 138205. doi:10.1016/j.jclepro.2023.138205.

[20] Na, S., Lee, S., & Youn, S. (2021). Experiment on activated carbon manufactured from waste coffee grounds on the compressive strength of cement mortars. Symmetry, 13(4), 619. doi:10.3390/sym13040619.

[21] Mohamed, G., & Djamila, B. (2018). Properties of dune sand concrete containing coffee waste. MATEC Web of Conferences, 149, 01039. doi:10.1051/matecconf/201814901039.

[22] Horma, O., Channouf, S., El Hammouti, A., El Hassani, S., Miri, H., Moussaoui, M. A., & Mezrhab, A. (2024). Enhancing concrete sustainability using crushed peanut shells: An analysis of thermophysical properties, durability, and application potential in construction. Journal of Building Engineering, 90. doi:10.1016/j.jobe.2024.109434.

[23] Sani, J. E., Goddey, O. A., Kevin, O. K., & Anthony, R. (2023). Durability of concrete made with groundnut shell ash as cement replacement. Materials Today: Proceedings, 86, 145–149. doi:10.1016/j.matpr.2023.05.218.

[24] Usman, J., Yahaya, N., & Mohammed Mazizah, E. (2019). Influence of groundnut shell ash on the properties of cement pastes. IOP Conference Series: Materials Science and Engineering, 601(1), 12015. doi:10.1088/1757-899X/601/1/012015.

[25] Shcherban', E. M., Stel'makh, S. A., Beskopylny, A. N., Mailyan, L. R., Meskhi, B., Chernil'nik, A., El'shaeva, D., Pogrebnyak, A., & Yaschenko, R. (2024). Influence of Sunflower Seed Husks Ash on the Structure Formation and Properties of Cement Concrete. Civil Engineering Journal (Iran), 10(5), 1475–1493. doi:10.28991/CEJ-2024-010-05-08.

[26] Afzal Basha, S., & Shaikh, F. U. A. (2023). Suitability of marble powders in production of high strength concrete. Low-Carbon Materials and Green Construction, 1(1), 27. doi:10.1007/s44242-023-00029-z.

[27] Shooshpasha, I., Hasanzadeh, A., & Kharun, M. (2020). Effect of silica fume on the ultrasonic pulse velocity of cemented sand. Journal of Physics: Conference Series, 1687(1), 012017. doi:10.1088/1742-6596/1687/1/012017.

[28] Shooshpasha, I., Hasanzadeh, A., & Kharun, M. (2019). The influence of micro silica on the compaction properties of cemented sand. IOP Conference Series: Materials Science and Engineering, 675(1), 12002. doi:10.1088/1757-899X/675/1/012002.

[29] Pereira, P., Evangelista, L., & De Brito, J. (2012). The effect of superplasticizers on the mechanical performance of concrete made with fine recycled concrete aggregates. Cement and Concrete Composites, 34(9), 1044–1052. doi:10.1016/j.cemconcomp.2012.06.009.

[30] Puertas, F., Santos, H., Palacios, M., & Martínez-Ramírez, S. (2005). Polycarboxylate superplasticiser admixtures: effect on hydration, microstructure and rheological behaviour in cement pastes. Advances in Cement Research, 17(2), 77-89. doi:10.1680/adcr.17.2.77.65044.

[31] Alsharari, F. (2025). Utilization of industrial, agricultural, and construction waste in cementitious composites: A comprehensive review of their impact on concrete properties and sustainable construction practices. Materials Today Sustainability, 29, 101080. doi:10.1016/j.mtsust.2025.101080.

[32] Ünal, M. T., Hashim, H., Gökçe, H. S., Ayough, P., Köksal, F., El-Shafie, A., & Salman, A. M. (2024). Physical and mechanical properties of pre-treated plant-based lightweight aggregate concretes: A review. Construction and Building Materials, 444, 137728. doi:10.1016/j.conbuildmat.2024.137728.

[33] Turk, O., Yehia, S., Abdelfatah, A., & Elchalakani, M. (2024). Sustainable concrete production: The potential of utilizing recycled waste materials. Journal of Building Engineering, 98, 111467. doi:10.1016/j.jobe.2024.111467.

[34] Haddadian, A., Johnson Alengaram, U., Ayough, P., Mo, K. H., & Mahmoud Alnahhal, A. (2023). Inherent characteristics of agro and industrial By-Products based lightweight concrete – A comprehensive review. Construction and Building Materials, 397, 132298. doi:10.1016/j.conbuildmat.2023.132298.

[35] GB/T 17671-1999. (1999), Method of Testing Cements-Determination of Strength. National Standards of the People's Republic of China, Beijing, China.

[36] ASTM C109/C109M-20. (2020). Standard Test Method for Compressive Strength of Hydraulic Cement Mortars (Using 2-in. or [50-mm] Cube Specimens). ASTM International, Pennsylvania, United States. doi:10.1520/C0109_C0109M-20.

[37] Haastrup, S., Bødker, M. S., Hansen, S. R., Yu, D., & Yue, Y. (2018). Impact of amorphous micro silica on the C-S-H phase formation in porous calcium silicates. Journal of Non-Crystalline Solids, 481, 556–561. doi:10.1016/j.jnoncrysol.2017.11.051.

[38] Yee, J. J., Khong, S. C., Tee, K. F., Jolius, G., & Chin, S. C. (2024). Spent coffee grounds enhanced compressive strength of cement mortar: an optimization study. Discover Applied Sciences, 6(7), 379. doi:10.1007/s42452-024-06077-9.

[39] Lee, J., Kim, J., & Lee, S. (2023). Study of Recycled Spent Coffee Grounds as Aggregates in Cementitious Materials. Recent Progress in Materials, 5(1), 1–23. doi:10.21926/rpm.2301007.

[40] Gwarah, L. S., Akatah, B. M., Onungwe, I., & Akpan, P. P. (2019). Partial Replacement of Ordinary Portland Cement with Sawdust Ash in Concrete. Current Journal of Applied Science and Technology, 4, 1–7. doi:10.9734/cjast/2019/v32i630036.

[41] Ikumapayi, C. M., Arum, C., & Alaneme, K. K. (2021). Reactivity and hydration behavior in groundnut shell ash based pozzolanic concrete. Materials Today: Proceedings, 38, 508–513. doi:10.1016/j.matpr.2020.02.385.

[42] Buari, T. A., Ademola, S. A., & Ayegbokiki, S. T. (2013). Characteristics Strength of groundnut shell ash (GSA) and Ordinary Portland cement (OPC) blended Concrete in Nigeria. IOSR Journal of Engineering, 3(7), 1-7. doi:10.9790/3021-03760107.

[43] Shahid, K. A., Ganesh, V., & Ghazali, N. (2024). The Incorporation of Spent Coffee Grounds as an Additive in Cement Ventilation Blocks. The Open Civil Engineering Journal, 18(1), 1-12. doi:10.2174/0118741495286280240206073611.

[44] Le, T. T., Park, S. S., Lee, J. C., & Lee, D. E. (2021). Strength characteristics of spent coffee grounds and oyster shells cemented with GGBS-based alkaline-activated materials. Construction and Building Materials, 267, 120986. doi:10.1016/j.conbuildmat.2020.120986.